The Journal of Immunology

RESEARCH ARTICLE | JULY 15 2022

Acetylcholine, Fatty Acids, and Lipid Mediators Are Linked to COVID-19 Severity

Malena M. Pérez; ... et. al

J Immunol (2022) 209 (2): 250–261.
https://doi.org/10.4049/jimmunol.2200079

Acetylcholine, Fatty Acids, and Lipid Mediators Are Linked to COVID-19 Severity

Malena M. Pérez,[*,1] Vinícius E. Pimentel,[*,†,1] Carlos A. Fuzo,[*,1] Pedro V. da Silva-Neto,[*,‡,§,1] Diana M. Toro,[*,‡,§,1] Thais F. C. Fraga-Silva,[¶] Luiz G. Gardinassi,[‖] Camilla N. S. Oliveira,[*,‡] Camila O. S. Souza,[*,†] Nicola T. Torre-Neto,[#] Jonatan C. S. de Carvalho,[#] Thais C. De Leo,[*,‡] Viviani Nardini,[*] Marley R. Feitosa,[,††] Rogerio S. Parra,[**,††] José J. R. da Rocha,[**] Omar Feres,[**,††] Fernando C. Vilar,[††,‡‡] Gilberto G. Gaspar,[‡‡] Leticia F. Constant,[§§] Fátima M. Ostini,[§§] Augusto M. Degiovani,[§§] Alessandro P. Amorim,[§§] Angelina L. Viana,[¶¶] Ana P. M. Fernandes,[‖‖] Sandra R. Maruyama,[##] Elisa M. S. Russo,[*] Isabel K. F. M. Santos,[¶] Vânia L. D. Bonato,[¶] Cristina R. B. Cardoso,[*,2] Carlos A. Sorgi,[#,2] Marcelo Dias-Baruffi,[*,2] and Lúcia H. Faccioli[*,2]; on behalf of the ImmunoCOVID Brazilian Research Consortium[3]**

Lipid and cholinergic mediators are inflammatory regulators, but their role in the immunopathology of COVID-19 is still unclear. Here, we used human blood and tracheal aspirate (TA) to investigate whether acetylcholine (Ach), fatty acids (FAs), and their derived lipid mediators (LMs) are associated with COVID-19 severity. First, we analyzed the perturbation profile induced by SARS-CoV-2 infection in the transcriptional profile of genes related to the ACh and FA/LM pathways. Blood and TA were used for metabolomic and lipidomic analyses and for quantification of leukocytes, cytokines, and ACh. Differential expression and coexpression gene network data revealed a unique transcriptional profile associated with ACh and FA/LM production, release, and cellular signaling. Transcriptomic data were corroborated by laboratory findings: SARS-CoV-2 infection increased plasma and TA levels of arachidonic acid, 5-hydroxy-6*E*,8*Z*,11*Z*,14*Z*-eicosatetraenoic acid, 11-hydroxy-5*Z*,8*Z*,12*E*,14*Z*-eicosatetraenoic acid, and ACh. TA samples also exhibited high levels of PGE_2, thromboxane B_2, 12-oxo-5*Z*,8*Z*,10*E*,14*Z*-eicosatetraenoic acid, and 6-*trans*-leukotriene B_4. Bioinformatics and experimental approaches demonstrated robust correlation between transcriptional profile in Ach and FA/LM pathways and parameters of severe COVID-19. As expected, the increased neutrophil-to-lymphocyte ratio, neutrophil counts, and cytokine levels (IL-6, IL-10, IL-1β, and IL-8) correlated with worse clinical scores. Glucocorticoids protected severe and critical patients and correlated with reduced Ach levels in plasma and TA samples. We demonstrated that pulmonary and systemic hyperinflammation in severe COVID-19 are associated with high levels of Ach and FA/LM. Glucocorticoids favored the survival of patients with severe/critical disease, and this effect was associated with a reduction in ACh levels. ***The Journal of Immunology*****, 2022, 209: 250–261.**

Severe acute respiratory syndrome coronavirus 2–infected individuals may be asymptomatic or present clinical manifestations ranging from acute respiratory distress syndrome to systemic hyperinflammation and organ failure. These events have been attributed mostly to cytokine storm, diffuse alveolar damage immunopathology, and viral load (1–5). However, autopsies of deceased patients with COVID-19 suggest that immune mediators other than cytokines contribute to their persistent systemic inflammation (6).

Bioactive lipids (oxylipins) perform several biological functions (7), and bioactive lipid mediators (LMs) derived from arachidonic acid (AA) metabolism, especially eicosanoids, are efficient biomarkers of protection (8) or severity in inflammation (9, 10), including respiratory diseases (7, 11). High concentrations of eicosanoids were detected in the bronchoalveolar lavage (BAL) of patients with SARS-CoV-2 infection, suggesting the participation of LMs in COVID-19 (12).

A publication from our laboratory has reported the essential role PGE_2 signaling via EP2/4 receptors in the excessive acetylcholine (ACh) release associated with cardiac dysfunction (10). This correlation between ACh and PGE_2 also occurs in vascular inflammation associated with hypertension (13). Interestingly, ACh is involved in Takotsubo syndrome, an inflammatory heart disease associated with COVID-19 (14, 15). ACh is a neurotransmitter released by the sympathetic and parasympathetic systems (16) that can also be produced by leukocytes (17) and airway epithelial cells (18). In addition, ACh regulates metabolism (19), cardiac function (20), airway inflammation (21), and cytokine production (22).

Despite the recent advances in understanding COVID-19, the role of LMs and ACh in the immunopathology of the disease still needs to be clarified. Here, we conducted a multifaceted study that included blood transcriptome, lipidomic, and metabolomic analyses, as well as ACh quantification in plasma and tracheal aspirates (TAs) from patients at different clinical stages of the disease. Our findings demonstrated a robust correlation between elevated levels of ACh and fatty acids (FAs)/LMs with the severity of COVID-19.

Materials and Methods

Ethical considerations

The participants included in the study signed the informed consent form elaborated according to the National Council on Human Research and the research ethics committee of the Faculdade de Ciências Farmacêuticas de Ribeirão Preto da Universidade de São Paulo. The approved protocol (Certificate of Ethics Presentation and Appreciation CAAE: 30525920.7.0000.5403). All participants were older than age 16 y and were selected according to the inclusion and dichotomization criteria of the World Health Organization adapted

www.jimmunol.org/cgi/doi/10.4049/jimmunol.2200079

according to support ventilation and oxygen requirement, as indicated in Supplemental Table I. Demographic and laboratory and clinical findings data from all participants in this study are provided in the supplemental material.

Study design and blood collection

This is an observational and descriptive study conducted from June 2020 to January 2021. After the admission procedure, blood samples were collected in the first 24 h from patients with COVID-19 (n = 195) who had positive nasopharyngeal swab results from RT quantitative PCR and/or serological assays to detect anti–SARS-CoV-2 IgM/IgG/IgA. Participants with COVID-19 who received care at two medical centers upon spontaneous demand were classified as asymptomatic to mild (Asy-to-mild; n = 36), moderate (n = 50), severe (n = 54), or critical (n = 55). Criteria for clinical classification of patients were defined at the time of sample collection. We used two control groups: those who were SARS-CoV-2-negative (healthy participants; n = 46) and hospitalized intubated donors negative for SARS-CoV-2 (critical control patients; n = 13). The critical control patients were intubated for different clinical primary conditions as indicated in the supplemental material. Blood samples from healthy control subjects and from Asy-to-mild, nonhospitalized participants were collected at the Centro de Desenvolvimento Científico e Tecnológico, Parque Supera (Ribeirão Preto, São Paulo, Brazil) or at the residence of the patients assisted by the Brazilian Public Health System (Sistema Único de Saúde). Blood examinations of healthy participants and nonhospitalized patients were performed at the Serviço de Análises Clínicas, Faculdade de Ciências Farmacêuticas de Ribeirão Preto, Universidade de São Paulo, Ribeirão Preto, São Paulo, Brazil. Clinical laboratory data included markers of liver and kidney function, cardiac enzymes, coagulation factors, RBCs, hemoglobin, platelets, and total and differential leukocytes in the blood samples. Plasma was separated from whole blood samples and stored at −80°C for cytokine and ACh measurement. For lipidomic and metabolomic analyses, plasma samples were immediately diluted in methanol (1:1 v/v) and stored at −80°C.

Tracheal aspirate collection and processing

Tracheal aspirate (TA) samples were collected from hospitalized COVID-19 critical patients (n = 38) and critical control subjects (n = 13). TA samples were collected as described before (23) and processed, and cell-free supernatant was used for lipidomic and metabolomic analyses and cytokine and ACh quantification. After counting total cells, the leukocyte numbers were adjusted to 1×10^9 cells/L for differential counts in cytospin preparations.

Transcriptomic analysis

To investigate the impact of ACh- and FA-related pathways on the gene expression perturbation in COVID-19, we analyzed transcriptomic data from the participants' whole blood leukocytes deposited on the ArrayExpress database at EMBL-EBI (www.ebi.ac.uk/arrayexpress) under accession number E-MTAB-11240. Sixty-six samples were distributed into five groups according to hospitalization and clinical classification: healthy participants (n = 12); Asy-to-mild patients (n = 12), moderate care patients (moderate) (n = 8), moderate hospitalized patients (n = 6), severe patients (n = 14), and critical patients (n = 14). We targeted the analysis on two lists of ACh- and FA-related genes obtained from the Reactome pathways (supplemental material). Characterization of transcript perturbation and association with patients' data were performed with base R functions, PCATools, and sjPlot. Differential expression analyses between previously described clinical groups were performed with limma using age, sex, body mass index (BMI), hypertension, diabetes, and outcome as covariates. Pathway overrepresentation was performed with clusterProfiler on Reactome pathways. A network based on the Spearman correlation was constructed, analyzed, and graphically represented using the R packages igraph, Intergraph, and ggnetwork. Other graphical representations were plotted using ggplot2 and pheatmap. We used

*Departamento de Análises Clínicas, Toxicológicas e Bromatológicas, Faculdade de Ciências Farmacêuticas de Ribeirão Preto, Universidade de São Paulo, Ribeirão Preto, São Paulo, Brazil; †Programa de Pós-Graduação em Imunologia Básica e Aplicada, Faculdade de Medicina de Ribeirão Preto, Universidade de São Paulo, Ribeirão Preto São Paulo, Brazil; ‡Programa de Pós-Graduação em Biociências e Biotecnologia Aplicadas à Farmácia, Faculdade de Ciências Farmacêuticas de Ribeirão Preto, Universidade de São Paulo, Ribeirão Preto, São Paulo, Brazil; §Programa de Pós-graduação em Imunologia Básica e Aplicada, Instituto de Ciências Biológicas, Universidade Federal do Amazonas, Manaus, Amazonas, Brazil; ¶Departamento de Bioquímica e Imunologia, Faculdade de Medicina de Ribeirão Preto, Universidade de São Paulo, São Paulo, Brazil; ‖Instituto de Patologia Tropical e Saúde Pública, Universidade Federal de Goiás, Goiânia, Goiás, Brazil; #Departamento de Química. Faculdade de Filosofia, Ciências e Letras de Ribeirão Preto, Universidade de São Paulo, Ribeirão Preto, São Paulo, Brazil; **Departamento de Cirurgia e Anatomia, Faculdade de Medicina de Ribeirão Preto, Universidade de São Paulo, Ribeirão Preto, São Paulo, Brazil; ††Hospital São Paulo, Ribeirão Preto, São Paulo, Brazil; ‡‡Departamento de Clínica Médica, Faculdade de Medicina de Ribeirão Preto, Universidade de São Paulo, São Paulo, Brazil; §§Hospital Santa Casa de Misericórdia de Ribeirão Preto, Ribeirão Preto, São Paulo, Brazil; ¶¶Departamento de Enfermagem Materno-Infantil e Saúde Pública, Escola de Enfermagem de Ribeirão Preto, Universidade de São Paulo, Ribeirão Preto, São Paulo, Brazil; ‖‖Departamento de Enfermagem Geral e Especializada, Escola de Enfermagem de Ribeirão Preto, Universidade de São Paulo, Ribeirão Preto, São Paulo, Brazil; ##Departamento de Genética e Evolução, Centro de Ciências Biológicas e da Saúde Universidade Federal de São Carlos, São Carlos, São Paulo, Brazil

[1]M.M.P., V.E.P., C.A.F., P.V.d.S.-N., and D.M.T. contributed equally to this work.

[2]C.R.B.C., C.A.S., M.D.-B., and L.H.F. are senior authors who contributed equally to this work.

[3]All authors and their affiliations appear at the end of this article.

ORCIDs: 0000-0003-3411-1545 (V.E.P.); 0000-0002-1003-3848 (D.M.T.); 0000-0002-2053-8938 (T.F.C.F.-S.); 0000-0002-9027-2688 (L.G.G.); 0000-0002-6922-5270 (C.O.S.S.); 0000-0001-8776-5417 (J.C.S.d.C.); 0000-0002-2741-089X (T.C.D.L.); 0000-0002-5092-3423 (V.N.); 0000-0002-5566-9284 (R.S.P.); 0000-0001-8232-5375 (F.C.V.); 0000-0002-4913-0370 (A.L.V.); 0000-0002-9274-7915 (E.M.S.R.); 0000-0002-2039-1884 (M.D.-B.); 0000-0002-4999-8305 (L.H.F.).

Received for publication January 26, 2022. Accepted for publication April 25, 2022.

This work was supported by São Paulo Research Foundation (Fundação de Amparo a Pesquisa do Estado de São Paulo) Grants #2020/05207-6, #2014/07125-6, and #2015/00658-1 to L.H.F.; #2020/08534-8 to M.M.P.; #2018/22667-0 to C.O.S.S.; #2021/04590-3 to C.A.S.; and #2020/05270-0 to V.L.D.B. Additional support was provided by Conselho Nacional de Desenvolvimento Científico e Tecnológico Grants #303259/2020-5-CNPq to L.H.F., #312606/2019-2-CNPq to M.D.-B., and #309583/2019-5-CNPq to C.R.B.C. Support was also provided by Coordenação de Aperfeiçoamento de Pessoal de Nível Superior (CAPES-Finance Code 001) and Pró-Reitora de Pesquisa da Universidade de São Paulo Grant USP-VIDA.

C.A.S., C.R.B.C., E.M.S.R., L.H.F., M.D.-B., A.P.M.F., and A.L.V. coordinated the collection of samples and were involved with ethical approval. V.E.P., C.N.S.O., P.V.d.S.-N., M.M.P., D.M.T., N.T.T.-N., and J.C.S.d.C. applied the clinical questionnaire by telephone survey, screened patients and volunteers, and organized the database. C.A.S. supervised the collection of home patients and healthy participants. C.A.S., A.P.M.F., A.L.V., P.V.d.S.-N., J.C.S.d.C., V.E.P., D.M.T., C.N.S.O., L.F.C., A.M.D., A.P.A., F.M.O., M.R.F., R.S.P., F.C.V., G.G.G., J.J.R.d.R., and O.F. performed or supported the sample collection from patients with COVID-19 and healthy participants. P.V.d.S.-N., V.E.P., T.F.C.F.-S., J.C.S.d.C., D.M.T., and C.N.S.O. performed sample fractionation, processing, and storage. M.M.P., V.E.P., P.V.d.S.-N., C.N.S.O., L.H.F., M.D.-B., N.T.T.-N., and D.M.T. collected the clinical data, performed demographic analysis, categorized participants, and classified patients' clinical scores. M.M.P., V.E.P., N.T.T.-N., and D.M.T. carried out mass spectrometry processes of purification of the samples. C.A.S., M.M.P., and V.N. performed formal analyses. M.M.P. and V.E.P. processed the samples and measured Ach. C.R.B.C., T.F.C.F.-S., C.O.S.S., and C.N.S.O. performed cytokine quantification. C.A.F., T.F.C.F.-S., T.C.D.L., V.L.D.B., and M.D.-B. performed the analysis of the transcriptome, including data analysis and interpretation, preparation of figures and tables, and the writing of these findings. L.G.G. and C.O.S.S. performed metabolomic analysis and prepared the metabolome figures. M.M.P., V.E.P., P.V.d.S.-N., D.M.T., C.N.S.O., M.D.-B., and C.A.F. performed the statistical analysis and built the graphs. V.E.P., M.M.P., P.V.d.S.-N., C.A.F., and D.M.T. construct the figures. L.H.F., M.D.-B., M.M.P., V.E.P., C.A.S., C.R.B.C., P.V.d.S.-N., and C.A.F. wrote the original draft. V.E.P., M.M.P., P.V.d.S.-N., M.D.-B., L.H.F., and C.A.S. created and organized the supplemental material. L.H.F., M.D.-B., I.K.F.M.S., and V.L.D.B. provided materials, equipment, and resources. L.H.F., C.A.S., C.R.B.C., V.L.D.B., M.D.-B., E.M.S.R., A.P.M.F., A.L.V., S.R.M., and I.K.F.M.S. coordinated the ImmunoCOVID Brazilian Research Consortium, designed the study, and performed a critical review of the manuscript. M.M.P., V.E.P., P.V.d.S.-N., C.A.F., D.M.T., C.R.B.C., C.A.S., E.M.S.R., M.D.-B., and L.H.F. edited the final manuscript. All authors read and approved the final version of the manuscript and the supplemental material.

Address correspondence and reprint requests to Prof. Lúcia Helena Faccioli or Dr. Marcelo Dias-Baruffi, Departamento de Análises Clínicas, Toxicológicas e Bromatológicas, Faculdade de Ciências Farmacêuticas de Ribeirão Preto, Universidade de São Paulo, Avenida do Café s/n, Ribeirão Preto, São Paulo 14040-903, Brazil. E-mail addresses: faccioli@fcfrp.usp.br (L.H.F.) or mdbaruff@fcfrp.usp.br (M.D.B.).

The online version of this article contains supplemental material.

Abbreviations used in this article: AA, arachidonic acid; ACh, acetylcholine; ACN, acetonitrile; Asy-to-mild, asymptomatic to mild; BMI, body mass index; CI, confidence interval; FA, fatty acid; FDR, false discovery rate; GC, glucocorticoid; 5-HETE, 5-hydroxy-6*E*, 8*Z*, 11*Z*, 14*Z*-eicosatetraenoic acid; 11-HETE, 11-hydroxy-5*Z*, 8*Z*12*E*, 14*Z*-eicosatetraenoic acid; 12-HETE, 12-hydroxy-5*Z*, 8*Z*, 10*E*, 14*Z*-eicosatetraenoic acid; 15-HETE, 15-hydroxy-5*Z*, 8*Z*, 11*Z*, 13*E*-eicosatetraenoic acid; LM, lipid mediator; LTB_4, leukotriene B_4; NLR, neutrophil-to-lymphocyte ratio; OR, odds ratio; 5-oxo-ETE, 5-oxo-6*E*, 8*Z*, 11*Z*, 14*Z*-eicosatetraenoic acid; 12-oxo-ETE, 12-oxo-5*Z*, 8*Z*, 10*E*, 14*Z*-eicosatetraenoic acid; 15-oxo-HETE, 15-oxo-hydroxyeicosatetraenoic acid; PC, principal component; TA, tracheal aspirate; TXB_2, thromboxane B_2.

other publicly available RNA-sequencing transcriptome datasets of whole blood leukocytes from patients with COVID-19 and non–COVID-19 individuals obtained from the Gene Expression Omnibus repository (https://www.ncbi.nlm.nih.gov/geo/) under accession number GSE157103 to investigate the consistency of transcriptional changes detected after analysis of our reference transcriptome data. We extracted two extreme conditions to perform differential expression analysis by asking for changes in patients with COVID-19 with mechanical ventilation and intensive care unit support (n = 42), and non–COVID-19 and non–intensive care unit patients (n = 10). Differentially expressed genes (DEGs) were defined on the basis of Benjamini and Hochberg–adjusted p values <0.05 to control for false discovery.

HPLC tandem mass spectrometry (LC-MS/MS)

Reagents. Eicosanoids, free FAs (AA, eicosapentaenoic acid, and docosahexaenoic acid), and metabolites as mol. wt. standards and deuterated internal standards were purchased from Cayman Chemical Co. (Ann Arbor, MI). HPLC-grade acetonitrile (ACN), methanol (MeOH), and isopropanol were purchased from Merck (Kenilworth, NJ). Ultrapure deionized water (H_2O) was obtained using the Milli-Q water purification system (Merck-Millipore, Kenilworth, NJ). Acetic acid and ammonium hydroxide were obtained from Sigma-Aldrich (St. Louis, MO).

Sample preparation and extraction. The plasma (250 μl) in EDTA-containing tubes (Vacutainer EDTA K2; BD Diagnostics, Franklin Lakes, NJ) and TA (250 μl) samples were stored in MeOH (1:1 v/v) at −80°C. Three additional volumes of ice-cold absolute MeOH were added to each sample for protein denaturation during 18 h at −20°C. To each sample, 10 μl of internal standard solution was added and centrifuged at 800 × g for 10 min at 4°C. The resulting supernatants were collected and diluted with deionized water (ultrapure water; Merck-Millipore, Kenilworth, NJ) to obtain 10% MeOH (v/v) of final concentration. In the solid phase extraction, a Hypersep C18 500-mg column (3 ml) (Thermo Scientific, Bellefonte, PA) equipped with an extraction manifold collector (Waters, Milford, MA) was used. The diluted samples were loaded into the preequilibrated column and washed using 2 ml of MeOH and H_2O containing 0.1% acetic acid, respectively. Then, the cartridges were flushed with 4 ml of H_2O containing 0.1% acetic acid to remove hydrophilic impurities. The lipids that had been adsorbed on the solid phase extraction sorbent were eluted with 1 ml of MeOH containing 0.1% acetic acid. The eluate solvent was removed in a vacuum (Concentrator Plus, Eppendorf, Germany) at room temperature and reconstituted in 50 μl of MeOH/H_2O (7:3 v/v) for LC-MS/MS analysis.

LC-MS/MS analysis and lipid data processing. LC was performed using an Ascentis Express C18 column (Supelco, St. Louis, MO) with the length of 100 mm, inner diameter 4.6 mm, and a particle size of 2.7 μm in an HPLC system (Nexera ×2; Shimadzu, Kyoto, Japan). Then, 20 μl of extracted sample was injected into the HPLC column. Elution was carried out under a binary gradient system consisting of phase A, composed of H_2O, ACN, and acetic acid (69.98:30:0.02 v/v/v) at pH 5.8 (adjusted with ammonium hydroxide), and phase B, composed of ACN and isopropanol (70:30 v/v). Gradient elution was performed for 25 min at a flow rate of 0.5 ml/min. The gradient conditions were as follows: 0 to 2 min, 0% B; 2 to 5 min, 15% B; 5 to 8 min, 20% B; 8 to 11 min, 35% B; 11 to 15 min, 70% B; and 15 to 19 min, 100% B. At 19 min, the gradient was returned to the initial condition of 0% B, and the column was reequilibrated until 25 min. During analysis, the column samples were maintained at 25°C and 4°C in the autosampler. The HPLC system was directly connected to a TripleTOF 5600$^+$ mass spectrometer (AB SCIEX, Foster City, CA). An electrospray ionization source in negative ion mode was used for high-resolution multiple-reaction monitoring scanning. An atmospheric pressure chemical ionization probe was used for external calibrations of the calibrated delivery system. Automatic mass calibration (<2 ppm) was performed periodically after each of the five sample injections using atmospheric pressure chemical ionization probe negative calibration solution (AB SCIEX, Foster City, CA) injected via direct infusion at a flow rate of 300 μl/min. Additional instrumental parameters were as follows: nebulizer gas, 50 ψ; turbo gas, 50 ψ; curtain gas, 25 ψ; electrospray voltage, −4.0 kV; temperature of the turbo ion spray source, 550°C. The dwell time was 10 ms, and a mass resolution of 35,000 was achieved at a mass-to-charge ratio (m/z) of 400. Data acquisition was performed using Analyst software (AB SCIEX, Foster City, CA). Qualitative identification of the lipid species was performed using PeakView (AB SCIEX, Foster City, CA). MultiQuant (AB SCIEX, Foster City, CA) was used for the quantitative analysis, which allows the normalization of the peak intensities of individual molecular ions using an internal standard for each class of lipid. Each compound was quantified using internal standards and calibration curves, and the specific mass transitions of each lipid were determined according to our previously published method (24) (supplemental material). The final concentration of lipids was normalized by the initial volume of plasma or TA fluid (ng/ml).

Metabolomic analysis. Untargeted metabolomic data were analyzed as previously described by our group (25, 26). Briefly, metabolite was extracted, and samples were transferred to autosampler vials for LC-MS analysis using a TripleTOF5600$^+$ mass spectrometer (AB SCIEX, Foster City, CA) coupled to an ultra-HPLC system (Nexera ×2; Shimadzu, Kyoto, Japan). Reverse-phase chromatography was performed similarly to the lipid analyses above. Mass spectral data were acquired with negative electrospray ionization, and the full scan of m/z ranged from 100 to 1500. ProteoWizard software (27) was used to convert the wiff files into m/z XML files. Peak peaking, noise filtering, retention time, m/z alignment, and feature quantification were performed using apLCMS (28). Three parameters were used to define a metabolite feature: m/z, retention time (min), and intensity values. Data were $\log_2$ transformed, and only features detected in at least 50% of samples from one group were used in further analyses. Missing values were imputed using half the mean of the feature across all samples. Mummichog (version 2) was used for metabolic pathway enrichment analysis (mass accuracy <10 ppm) (29). Statistical analysis of untargeted metabolomic data was performed with the R package limma and moderated F-test.

Acetylcholine measurement. ACh was measured in heparinized plasma (SST Gel Advance; BD Diagnostics, Franklin Lakes, NJ) and in TA using a commercially available immunofluorescence kit (ab65345; Abcam, Cambridge, UK) according to the manufacturer's instructions. Briefly, ACh was converted to choline by adding the enzyme acetylcholinesterase to the reaction, which allows total and free choline measurement. The amount of ACh present in the samples was calculated by subtracting the free choline from the total choline. The products formed in the assay react with the choline probe and can be measured by fluorescence with excitation and emission wavelengths of 535 and 587 nm, respectively (Paradigm Plate Reader; SpectraMax, San Diego, CA). The concentration of ACh was analyzed using SoftMax software (SpectraMax, Molecular Devices, Sunnyvale, CA), expressed as pmol/ml.

Cytokine quantification. The cytokines IL-6, IL-8, IL-1β, IL-10, and TNF were quantified in heparinized plasma and TA fluid samples using a BD Cytometric Bead Array Human Inflammatory Kit (BD Biosciences, San Jose, CA), according to the manufacturer's instructions. Briefly, after sample processing, the cytokine beads were counted using a flow cytometer (FACSCanto II; BD Biosciences, San Jose, CA), and analyses were performed using FCAP Array (3.0) software (BD Biosciences, San Jose, CA). The concentrations of cytokines were expressed as pg/ml.

Statistical analysis. Normality of data distribution was analyzed using the Kolmogorov-Smirnov test. All analyses were performed using two-tailed tests, with a significance value of $p < 0.05$ and a 95% confidence interval (CI). Because the data did not have Gaussian distribution, they were analyzed using the Mann-Whitney test (to compare two groups) or the Kruskal-Wallis test, followed by Dunn's posttest to compare three or more groups. Spearman's correlation was performed to identify correlation between plasma and TA levels of ACh and FAs/LMs related to COVID-19 clinical parameters and laboratory findings. More specifically, the following parameters of patients with COVID-19 were used to construct the correlation matrix: the cytokines IL-1β, TNF, IL-10, IL-6, and IL-8; ACh; 5-hydroxy-6*E*,8*Z*,11*Z*,14*Z*-eicosatetraenoic acid (5-HETE), 11-hydroxy-5*Z*,8*Z*,12*E*,14*Z*-eicosatetraenoic acid (11-HETE), 12-oxo-5*Z*,8*Z*,10*E*,14*Z*-eicosatetraenoic acid (12-oxo-ETE), thromboxane B_2 (TXB_2), 5-oxo-6*E*,8*Z*,11*Z*,14*Z*-eicosatetraenoic acid (5-oxo-ETE), 15-hydroxy-5*Z*,8*Z*,11*Z*,13*E*-eicosatetraenoic acid (15-HETE), PGE_2, 6-*trans*-leukotriene B_4 (6-*trans*-LTB_4), 5*S*,12*R*-LTB_4, prostaglandin D_2, 15-oxo-hydroxyeicosatetraenoic acid (15-oxo-HETE), 12-hydroxy-5*Z*,8*Z*,10*E*,14*Z*-eicosatetraenoic acid (12-HETE); laboratory tests, including whole blood cells, WBCs, neutrophils, lymphocytes, platelets, International Standardized Index, urea, creatinine, lactate, and C-reactive protein; and the clinical characteristics severity, BMI, and days of hospitalization. The differences were considered statistically significant at $p < 0.05$.

Binomial logistic regression analysis was performed to examine the disease severity and death rate in patients with COVID-19 treated with glucocorticoids (GCs), ACh, and FA/LM using Jamovi Project (version 1.6, 2021); the model was adjusted by sex, BMI, and age for patient groups at different stages of the disease. Results were tabulated using GraphPad Prism software (version 9.0) and Project R. Transcriptomic and metabolomic data were analyzed using the software packages indicated in their respective sections.

Results

Modifications in acetylcholine and fatty acid–/lipid mediator–related gene expression are associated with COVID-19 severity

We analyzed blood transcriptomic data in 66 participants from our cohort (E-MTAB-11240). Comparative analysis of the first principal

component (PC1) of the total transcriptome PC analysis indicated that ACh and FA/LM-related genes figured out the SARS-CoV-2–induced gene perturbation. FA/LM genes were more strongly associated with COVID-19 severity gene signature than ACh genes (Fig. 1A). The multiple regression approach revealed positive associations of clinical scores and hypertension with PC1 variations in ACh and FA/LM gene sets; however, the impact of clinical scores was more robust (Fig. 1B). There was a strong positive association between PC1 variations in FA/LM gene sets and neutrophil-to-lymphocyte ratio (NLR) (Fig. 1B).

On the basis of a comparative analysis of all clinical groups taken in pairs, we detected 65 DEGs (11 for ACh and 54 for FA/LM) present in at least one clinical group (false discovery rate [FDR]-adjusted $p < 0.05$), which were clustered in downregulated (cluster 1) and upregulated (cluster 2) gene expression profiles relative to COVID-19 severity (Fig. 1C, supplemental material). Interestingly, we codetected DEGs related to ACh and FA pathways in both clusters, even considering subsequent roots in the clustering dendrogram; this transcriptional profile suggested crosstalk between ACh and FA/LM-related genes. The first two major terms in the enrichment analysis using the Reactome pathways of the DEGs were mitochondrial FA β-oxidation and eicosanoid receptor ligands for cluster 1 and AA metabolism, leukotriene, and eoxin synthesis for cluster 2 (supplemental material). We identified the DEGs with the most representative profiles of transcriptional variation associated with ACh (*SLC5A7*, *RIMS1*, *PTPRF*, *PPFIA2*, *UNC13B*, *GNAQ*, *CHRNA5*, *CHRM5*) and FA/LM pathways (*ALOX5AP*, *ALOX5*, *CYP1B1*, *MAPKAPK2*, *OLAH*, *LTB4R*, *THEM4*, *CYP4F2*, *CYP4F3*, *DPEP2*, *ACSL1*, *PTGS1*, *OXER1*, *HACL1*) in the supplemental material.

Correlation network analysis revealed a strong association between FA/LM and ACh pathway DEGs and COVID-19 severity parameters, such as clinical score and NLR (Fig. 1D, supplemental material). The upregulated expression of *ALOX5* and *ALOX5AP* genes demonstrated their central importance for network connectivity (Fig. 1D). Based on network data, four DEGs of the ACh pathway (*GNAQ*, *RIMS1*, *PPFIA2*, and *UNC13B*) were positively correlated with COVID-19 severity parameters. We also observed a strong correlation between *ALOX5* and *GNAQ* gene expression, which are involved in FA/LM metabolism and ACh cell signaling, respectively (Fig. 1D). However, downregulated DEGs were detected only in FA metabolism pathways (*THEM4* and *HACL1*) that were negatively correlated with clinical score and NLR (Fig. 1D).

To amplify the robustness of our transcriptome results, we analyzed other publicly available whole blood leukocytes RNA-sequencing transcriptome data from patients with COVID-19 and patients without COVID-19 (Gene Expression Omnibus accession no. GSE157103) (30). Interestingly, comparative analysis between the E-MTAB-11240 and GSE157103 transcriptome datasets indicated that in the set of 65 DEGs associated with the ACh and FA pathways detected in the individuals from our cohort, 32 DEGs were also detected in the GSE157103 dataset, and 26 exhibited the same pattern of gene regulation (supplemental material). This comparison reinforces the involvement of the ACh and FA/LM pathways in the transcriptional perturbation associated with COVID-19 severity.

The severity of COVID-19 correlates with increased levels of acetylcholine and fatty acids/lipid mediators

We analyzed blood samples from healthy participants and participants with COVID-19 to perform nontargeted metabolomic analysis. A total of 8791 metabolite features were present in at least 50% of all samples, and the relative abundance of 595 metabolite features (FDR-adjusted $p < 0.05$) was altered in the groups studied (Supplemental Fig. 1). Two-way hierarchical clustering based on significant metabolic features resulted in three well-differentiated clusters: one for healthy participants, one for patients with Asy-to-moderate COVID-19, and one for patients with severe/critical COVID-19 (Supplemental Fig. 1). Pathway analysis revealed that the main significant metabolic pathways are enriched in features involved in FA biosynthesis, metabolism, activation, and oxidation (Fig. 2A). Compared with healthy participants, patients with COVID-19 showed an increased abundance of FA, such as linoleic acid, tetradecanoate, and dodecanoate (Fig. 2B–D).

The analysis of TA metabolomes from hospitalized patients without COVID-19 and patients with critical COVID-19 showed distinct abundance of metabolic features between these groups (FDR-adjusted $p < 0.05$). Hierarchical analysis enabled the definition of different clusters that corresponded to metabolic features for critically ill patients with or without COVID-19 (Supplemental Fig. 1). SARS-CoV-2 infection induced changes in lung metabolism, as revealed by disturbances in sphingolipids, β-oxidation of trihydroxyprostanoyl-CoA, biosynthesis, and metabolism of steroid hormones, vitamin D_3, and glycerophospholipids (Fig. 2E). Interestingly, 25-hydroxyvitamin D_3 [25(OH)D_3], 24,25-dihydroxyvitamin D_3, and 23S,25,26-trihydroxyvitamin D_3 levels were higher in TAs from severe/critical patients than in critical control participants (Supplemental Fig. 1). In plasma lipidomic analysis, compared with healthy participants, patients with critical COVID-19 exhibited significantly higher levels of AA and 5-HETE, but 11-HETE levels in critical patients were significantly increased only when compared with patients with moderate COVID-19 (Fig. 2F–H). AA was the most abundant lipid identified, and its levels correlate with the COVID-19 severity.

When compared with critical control participants, patients with critical COVID-19 had augmented TA levels of AA, 12-oxo-ETE, 5-HETE, 6-*trans*-LTB_4, PGE_2, TXB_2, and 11-HETE (Fig. 2I). Our results showed that the metabolic pathways related to cyclooxygenase and lipoxygenase were more perturbed (5-HETE > TXB_2 > PGE_2 ≈ 12-oxo-ETE > 6-*trans*-LTB_4) in the TAs of patients with critical COVID-19 when compared with critical control participants. TAs and blood samples from patients with critical COVID-19 showed distinct profiles of FA/LM, demonstrating that markers of hyperinflammation in systemic and pulmonary microenvironments are not identical.

The absolute leukocyte and neutrophil counts, but not the lymphocyte counts, were significantly higher in patients with severe and critical COVID-19 than in healthy participants (Supplemental Fig. 2). Basophil and eosinophil counts were reduced in severe COVID-19 compared with Asy-to-moderate disease (Supplemental Fig. 2). Compared with healthy participants, patients with severe COVID-19 had similar whole blood monocyte counts and elevated platelet counts (Supplemental Fig. 2). We detected a significant increase in neutrophil counts from TAs of patients with critical COVID-19, as compared with critical control individuals, and lymphocyte numbers tended to be increased (Supplemental Fig. 2). Plasma cytokine quantification identified significant elevation in IL-8, IL-6, and IL-10 in patients with moderate, severe, and critical COVID-19 when compared with healthy participants. The IL-1β and TNF levels of critical patients resembled those of the remaining groups evaluated in this study (Supplemental Fig. 2). In contrast to the eicosanoids, critical patients with or without SARS-CoV-2 exhibited similar TA cytokine profiles (Supplemental Fig. 2).

Patients with critical COVID-19 exhibited significantly higher plasma ACh levels than healthy and asymptomatic participants, indicating that this marker increased with disease severity (Fig. 3A). Interestingly, patients with severe and critical COVID-19 treated with GCs exhibited significantly lower plasma ACh levels than non–GC-treated patients in the same clinical conditions (Fig. 3B). TA samples from non–GC-treated critical patients had ∼16-fold higher ACh levels than their plasma samples. Similar to what we

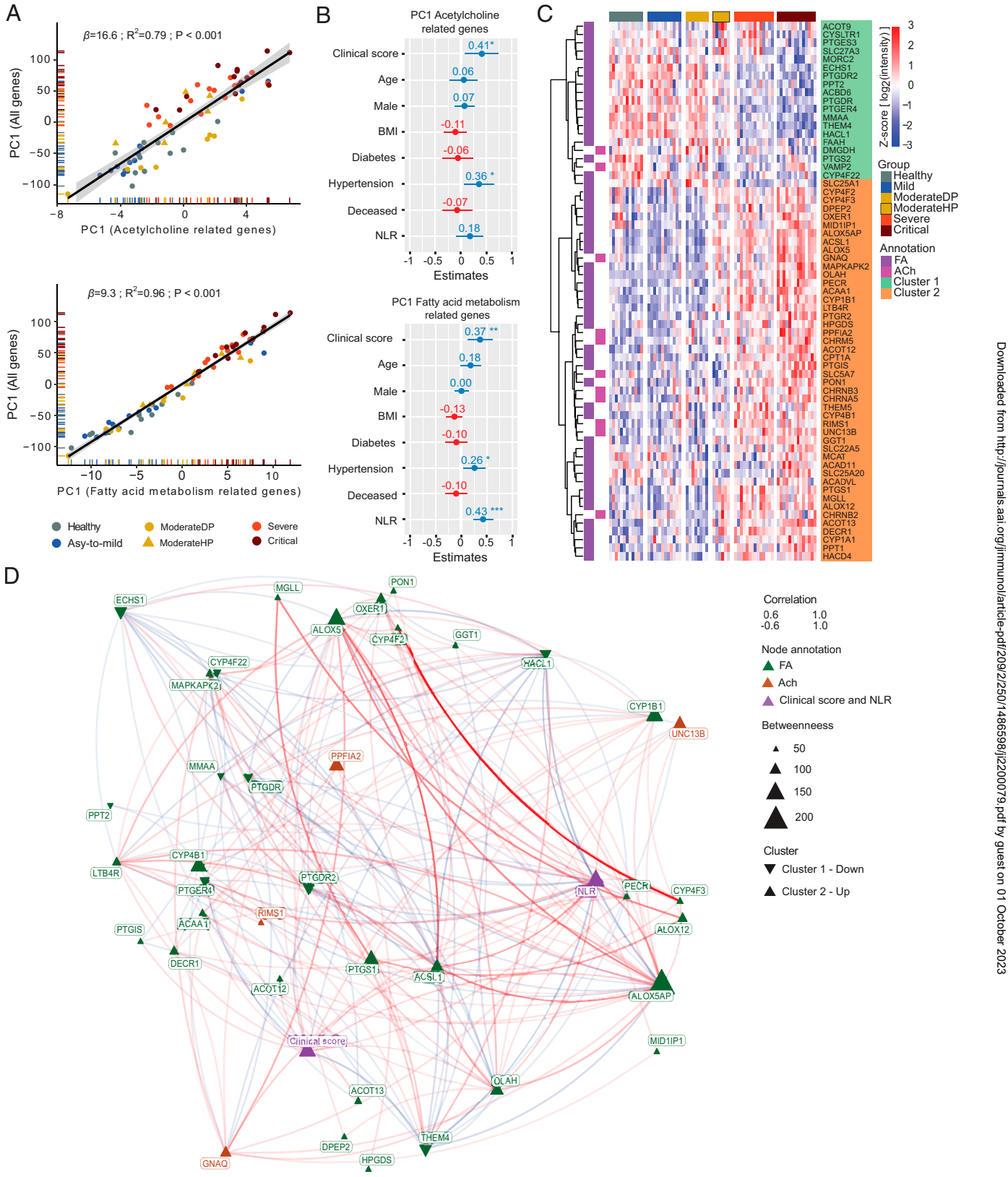

FIGURE 1. Variations in blood transcriptional profiles of ACh- and FA/LM-related genes are correlated with COVID-19 severity. (**A**) Linear regression analysis of the associations between PC1 and the variation in expression levels of transcripts of ACh- and FA/LM-related genes. (**B**) Forest plot for standardized β-coefficients obtained from multivariate linear regression analysis of the association between PC1 of ACh- and FA/LM-related genes and patients' data. *$p < 0.05$, **$p < 0.01$, ***$p < 0.001$. (**C**) Heatmap of DEGs (transcriptome-wide FDR-adjusted <0.05) across clinical groups, as determined using the limma protocol and the covariates age, sex, BMI, diabetes, hypertension, and outcome in the regression model. The samples and transcript expression were clustered using the Ward's minimum variance method with Euclidean distance. (**D**) Network of correlations among DEGs, clinical scores, and NLRs using circrand layout. The correlation pairs were selected based on absolute Spearman's rho >0.6 and $p < 0.05$. Triangles represent the nodes; their color represents the origin of DEG according to ACh or FA/LM; their size represents the betweenness centrality metric; and their up- and downsided orientation represents the normality and downregulation, respectively, of each cluster profile.

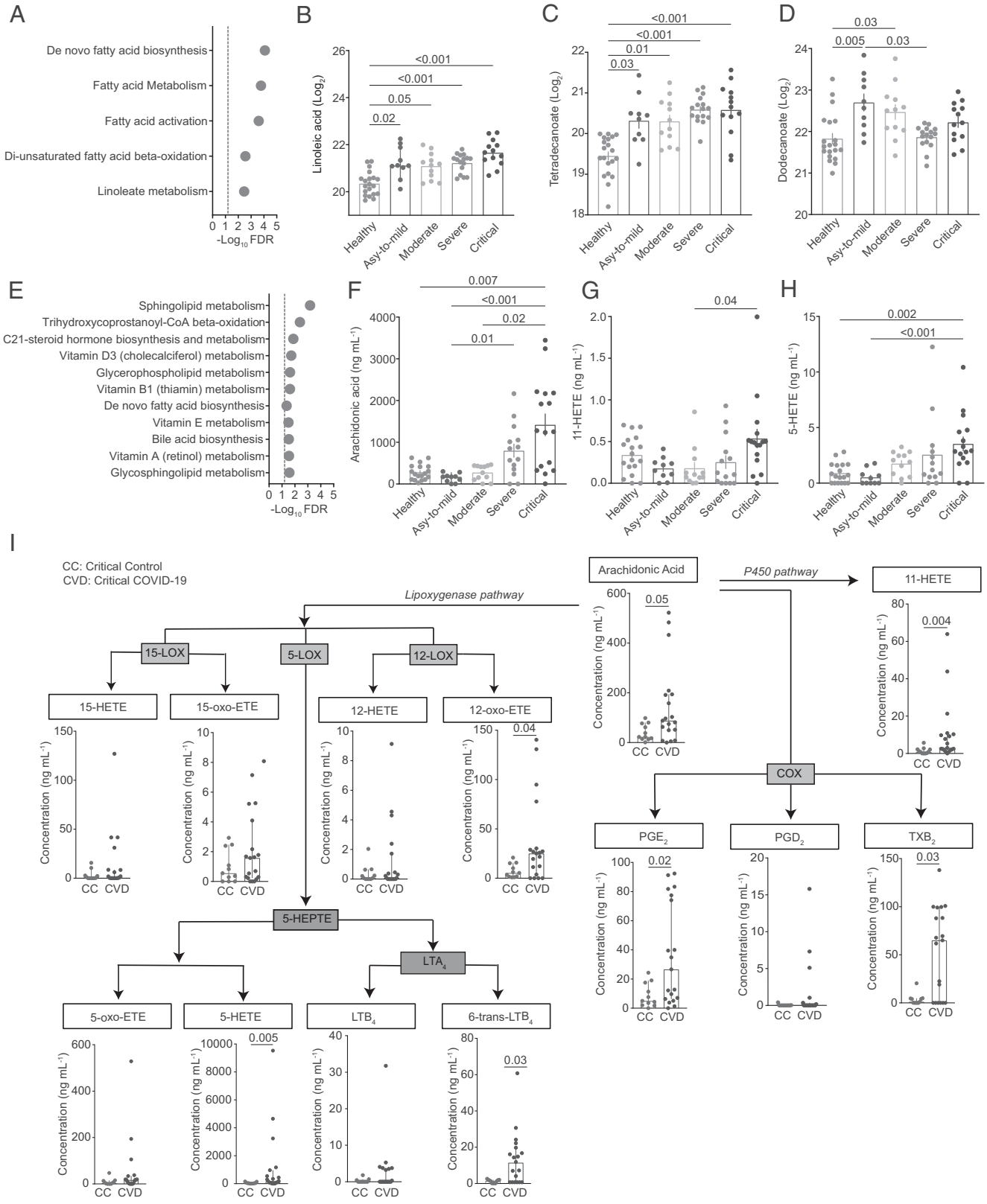

FIGURE 2. Metabolomic and lipidomic analyses reveal increased levels of free FAs and LMs in plasma samples and TAs from patients with COVID-19. Analysis of untargeted MS data demonstrated metabolic pathway enrichment in (**A**) plasma samples and (**E**) TAs. (**B**–**D**) Plasma metabolomics shows a significant increase of free FA levels in patients with COVID-19 ($n = 10$ asymptomatic; $n = 12$ moderate; $n = 16$ severe; $n = 13$ critical), as compared with healthy participants ($n = 20$). (E) TA metabolomics shows increased levels of sphingolipid metabolism, β-oxidation of trihydroxyprostanoil-CoA, biosynthesis and metabolism of steroidal hormones, vitamin D_3, and glycerophospholipids ($n = 13$ critical control participants; $n = 38$ patients with critical COVID-19). Differential abundance was calculated using the limma package for R, and FDR was controlled using the Benjamini-Hochberg method. Mummichog software version 2.3.3 was used for pathway enrichment analysis. (**F**–**H**) Plasma lipidomic analysis was performed using targeted MS, which confirmed the elevation of AA, 11-HETE, and 5-HETE according to COVID-19 severity ($n = 20$ healthy participants; $n = 10$ asymptomatic; $n = 12$ moderate; $n = 15$ severe; $n = 16$ critical). (**I**) Lipidomic analysis was performed using targeted MS and confirmed the elevation of LM derived *(Figure legend continues)*

detected in plasma samples, GC treatment completely inhibited ACh release in TA from critical individuals. Although ACh levels in non–GC-treated critical control participants were detected, the concentration was lower than those detected in patients with critical COVID-19 (Fig. 3C).

To understand whether the levels of FAs/LMs and ACh measured in plasma samples and TAs were associated with inflammatory biomarkers and/or clinical parameters of COVID-19, we performed Spearman's correlation analysis among pairs of these variables. In blood, all FAs/LMs detected (AA, 5-HETE, and 11-HETE) were strongly or moderately correlated with ACh. FA/LM and ACh concentrations were positively, moderately, or strongly correlated with disease severity, whereas 5-HETE and ACh levels correlated moderately with the patients' hospitalization period (Fig. 3D). Increased levels of FAs/LMs and ACh correlated positively in plasma samples that varied from weak to strong intensities with inflammatory or thrombotic markers, such as neutrophil counts, international normalized ratio, IL-1β, IL-6, and IL-8 (Fig. 3D).

In addition, high TA levels of AA, 5-HETE, and 12-HETE, from patients with critical COVID-19 positively correlated with the elevated BMI values, whereas 5-oxo-ETE showed a positive correlation with patients' hospitalization period (Fig. 3E). Furthermore, high ACh TA levels presented a high PGE_2 positive correlation, whereas IL-10 presented a negative correlation, in patients with critical COVID-19 (Fig. 3E).

Glucocorticoid therapy prevents severity and lethality in patients with COVID-19

To understand the effect of independent variables such as GC, AA, ACh, 5-HETE, and 11-HETE levels on the severity and outcome of COVID-19, a binomial logistic regression analysis was performed using a model adjusted for sex, BMI, and age. Considering that the statistical model included patients from moderate to critical groups, as well as the odds ratio (OR) and 95% CI, we identified beneficial effects of GC therapy related to disease progression and lethality, and this effect was more prominent in severe patients (Fig. 4A, 4B). Interestingly, this beneficial action of GC therapy was associated with reduced levels of ACh (death, GC, OR, 0.38; 95% CI, 0.002–0.6; $p = 0.021$; severity, GC, OR, 0.02; 95% CI, 0.001–0.48; $p = 0.015$). However, ACh levels did not show a significant association with both outcomes, and this event could be related to the inhibitory effect of GC therapy on ACh production (Fig. 4A–D). Although statistical analyses detected no significant differences, among the groups, they revealed that the independent variable 11-HETE had a tendency towards the risk of severity and death (death, 11-HETE, OR, 4.5; 95% CI, 0.24–86.0; $p = 0.307$; severity, 11-HETE, OR, 2.0; 95% CI, 0.002–1525.7; $p = 0.832$) (Fig. 4A, 4B).

Discussion

SARS-CoV-2 induces a hyperinflammation syndrome associated with metabolic alterations in the host, and it may favor viral infection (31). On the basis of our analyses of whole blood leukocyte transcriptome, laboratory findings, and clinical data, we demonstrated that the uncontrolled innate immune response induced by SARS-CoV-2 infection is associated with high FA/LM and ACh production, mainly in patients with severe and critical disease. Increased levels of FA/LM and ACh are also correlated in other inflammatory processes such as scorpion envenomation and hypertension (10, 32, 33).

The analysis of the whole blood leukocyte transcriptomic analysis of 66 patients in our cohort indicated that transcriptional disturbance associated with COVID-19 severity included alterations in the ACh and FA/LM pathways. In this sense, patients with severe and critical disease showed altered expression of genes related to synthesis, secretion, and cellular signaling of ACh and FA/LM. We detected upregulated genes encoding proteins involved in choline transport and synaptic vesicle exocytosis (*SLC5A7* and *UNC13B*), proinflammatory events associated with ACh cell signaling (*PPFIA2* and *GNAQ*) and enzymes of FA production derivatives (*ALOX5*, *ALOX5AP*, *PTGS1*, and *OLAH*), and expression of proinflammatory cholinergic and LM or eicosanoid receptors (*CHRM5*, *CHRNA5*, *OXER1*, and *LTB4R*). We also detected a strong reduction in the expression of two genes associated with FA metabolism (*THEM4* and *HACL1*) that encode proteins with anti-inflammatory properties (34, 35). The *HACL1* gene product regulates the peroxisome proliferator-activated receptor-α signaling pathway and impairs the endogenous production of odd-chain FA metabolites, which favors hyperinflammation and COVID-19 severity (34, 36–38). The *THEM4* gene product participates in the anti-inflammatory action of vitamin D by downmodulating synthesis of LM derived from the COX-2 pathway (39). In this sense, reduced expression of this gene in patients with COVID-19 restrains the beneficial effects of vitamin D in controlling disease progression.

Our findings suggest the existence of crosstalk between lipid and cholinergic mediators favoring COVID-19 severity. *GNAQ* mRNA upregulation is an excellent example of this event. It encodes the G protein–coupled receptor of the Gq/11 family that regulates both the signal transduction of muscarinic receptors involved in inflammatory processes (40) and the activity of phospholipase C-β (41), an enzyme that mediates the 1,2-diacylglycerol release and indirect increase of Ca^{2+} influx, leading to cytosolic phospholipase A_2 activation and high AA release in activated human neutrophils (42). Furthermore, laboratory findings together with transcriptomic data from our cohort supported the existence of an interface of neutrophilia with ACh/FA/LM pathways in COVID-19 severity. Reanalysis of public transcriptome data from hospitalized patients with and without COVID-19 (GSE157103) using DEGs identified in our transcriptome dataset reinforced our findings, showing that ACh and FA/LM pathways were involved in COVID-19 severity. The genes with similar expression profiles in both analyses were *GNAC*, *UNC13B*, *ALOX*-5, *ALOX5AP*, *THEM4*, *HACL1*, and *PTGS1*. Together, these data indicated that high levels of ACh and FA/LM, combined with high expression of their receptors associated with proinflammatory activities, contributed to COVID-19 immunopathology.

FA/LM metabolism is one of the most altered pathways during COVID-19 (43). These biomolecules, such as oleic acid, AA, and PGE_2, could actively participate in virus fusion with host cell membranes, endocytosis, viral replication, and inflammation induction (44). Our metabolomic analysis revealed that the profile of metabolic pathways in blood and TAs is related to the synthesis and

from AA metabolism by lipoxygenase (LOX), cyclooxygenase (COX) and P450 pathway in TAs from patients with critical COVID-19 ($n = 19$) as compared with critical control participants ($n = 11$). Blood was collected within the first 24 h of admission in the health care unit, and TAs were collected from intubated critical patients (median, 6 d) with a confirmed diagnosis of SARS-CoV-2 infection (critical COVID-19) and from intubated patients without SARS-CoV-2 infection (critical control). Statistics in B–D and F–G were calculated by ANOVA followed by Mann-Whitney posttest; statistics in I were calculated by Student *t* test; significance is indicated by bars where $p < 0.05$. The bars in B–D and F–I represent the median ± 95% CI, and the dots represent data dispersion.

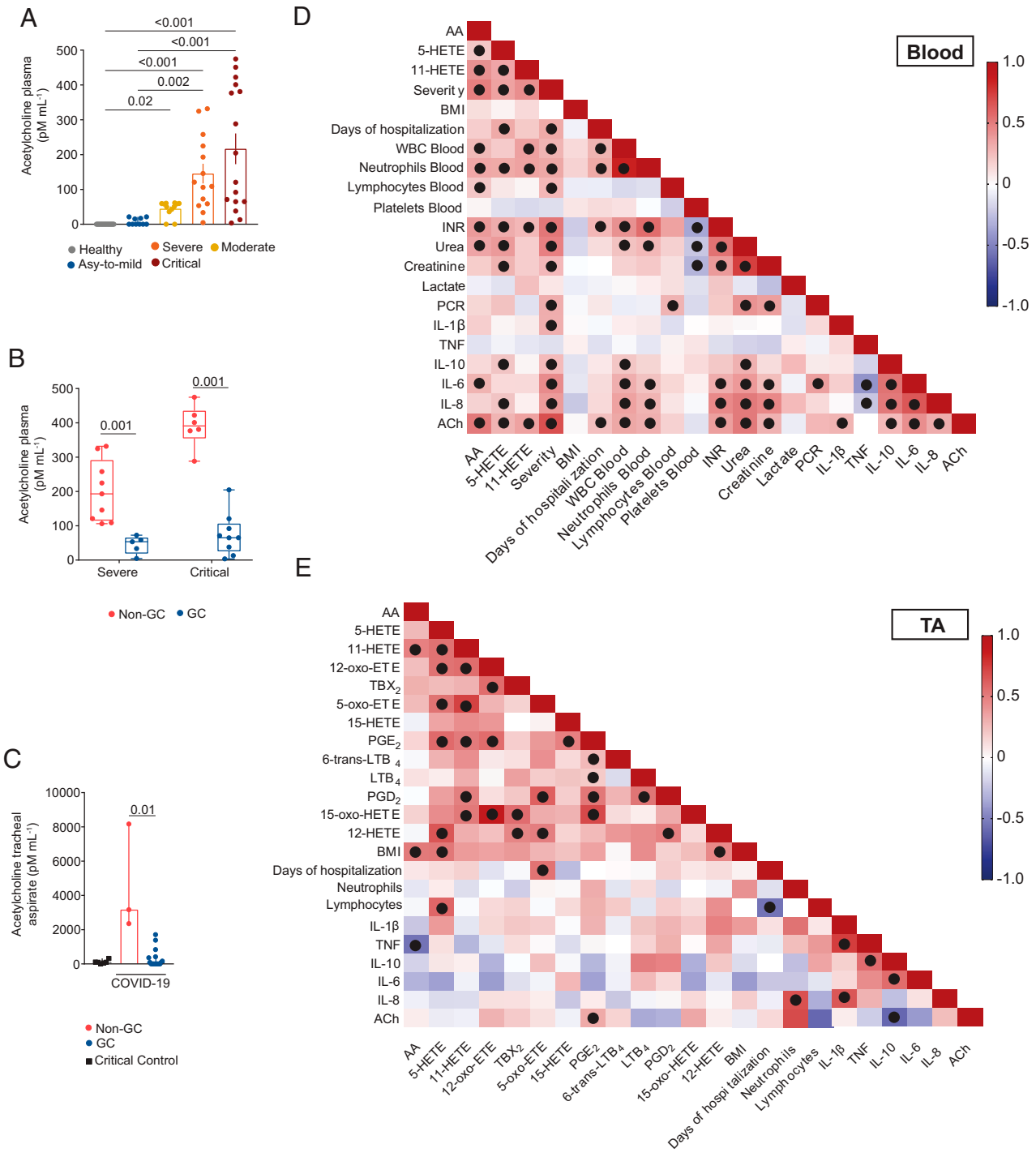

FIGURE 3. Severe and critical phases of COVID-19 are characterized by increased systemic and pulmonary release of ACh, which is inhibited by treatment with GCs and correlates with FA/LM levels and clinical parameters. (**A**) Compared with healthy participants ($n = 18$), plasma ACh concentration (pM/ml) was increased in SARS-CoV-2–infected patients according to disease severity ($n = 10$ asymptomatic; $n = 12$ moderate; $n = 14$ severe; $n = 16$ critical). (**B**) Treatment with GCs decreased plasma ACh concentration (pM/ml) in patients with severe ($n = 9$ non-GC; $n = 5$ GC) and critical ($n = 6$ non-GC; $n = 9$ GC) COVID-19. (**C**) Critical SARS-CoV-2–infected patients not treated with GCs ($n = 3$) exhibited increased TA ACh concentration (pM/ml) compared with critical patients treated with GCs ($n = 13$) and critical non–COVID-19 control participants ($n = 17$). (**D**) Spearman's correlation between plasma levels of FA/LM and ACh and COVID-19 clinical parameters ($n = 15$ moderate; $n = 27$ severe; $n = 22$ critical). (**E**) Spearman's correlation between TA levels of FA/LM and ACh and COVID-19 clinical parameters ($n = 18$ patients with critical COVID-19). Statistics in A and C were calculated by ANOVA followed by Mann-Whitney posttest, with significance indicated by bars, where $p < 0.05$; the bars represent the median ± 95% CI, and the dots represent data dispersion. Statistics in B were calculated by Mann-Whitney test, with significance indicated by bars, where $p < 0.05$. Statistics in D and E were calculated by the nonparametric Spearman's correlation matrix between the levels of FA/LM and ACh, and clinical parameters were plotted using the GraphPad Prism version 9.0 package. Red shades indicate positive correlations; blue shades represent negative correlations; black circles indicate $p < 0.05$, which was the threshold of significance. Blood and TA fluid were collected during hospitalization, on average, 6 to 17 d after admission. GCs (methylprednisolone from 40 to 500 mg/kg/d or dexamethasone from 1.5 to 6.0 mg/kg/d) were administered i.v.

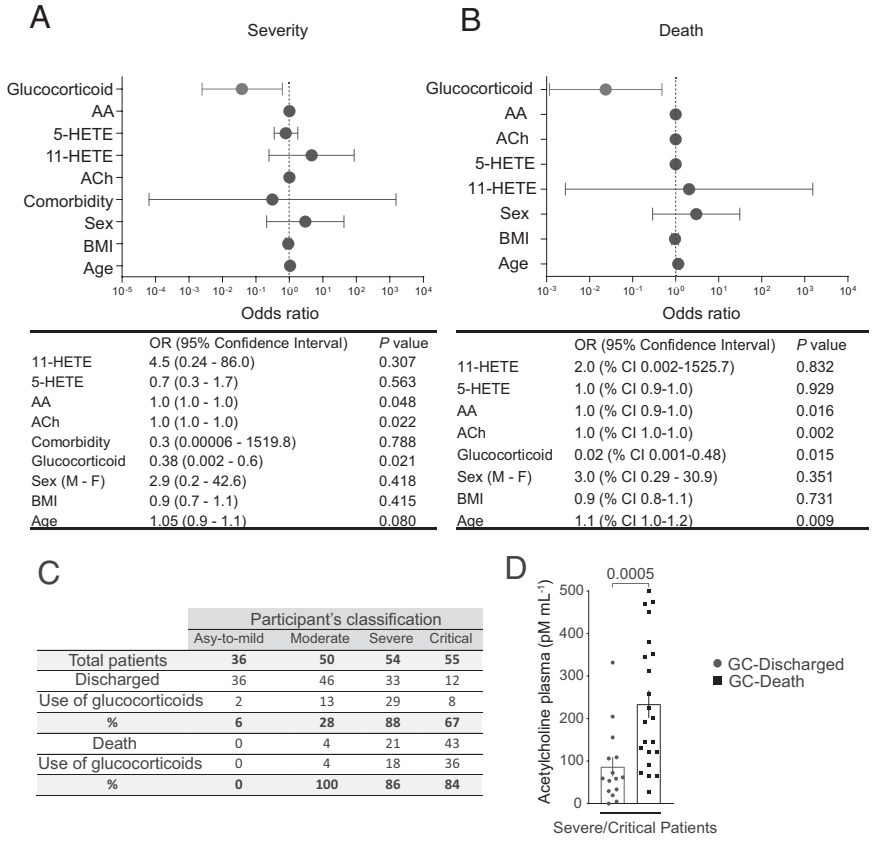

	OR (95% Confidence Interval)	*P* value
11-HETE	4.5 (0.24 - 86.0)	0.307
5-HETE	0.7 (0.3 - 1.7)	0.563
AA	1.0 (1.0 - 1.0)	0.048
ACh	1.0 (1.0 - 1.0)	0.022
Comorbidity	0.3 (0.00006 - 1519.8)	0.788
Glucocorticoid	0.38 (0.002 - 0.6)	0.021
Sex (M - F)	2.9 (0.2 - 42.6)	0.418
BMI	0.9 (0.7 - 1.1)	0.415
Age	1.05 (0.9 - 1.1)	0.080

	OR (95% Confidence Interval)	*P* value
11-HETE	2.0 (% CI 0.002-1525.7)	0.832
5-HETE	1.0 (% CI 0.9-1.0)	0.929
AA	1.0 (% CI 0.9-1.0)	0.016
ACh	1.0 (% CI 1.0-1.0)	0.002
Glucocorticoid	0.02 (% CI 0.001-0.48)	0.015
Sex (M - F)	3.0 (% CI 0.29 - 30.9)	0.351
BMI	0.9 (% CI 0.8-1.1)	0.731
Age	1.1 (% CI 1.0-1.2)	0.009

C

	Participant's classification			
	Asy-to-mild	Moderate	Severe	Critical
Total patients	**36**	**50**	**54**	**55**
Discharged	36	46	33	12
Use of glucocorticoids	2	13	29	8
%	**6**	**28**	**88**	**67**
Death	0	4	21	43
Use of glucocorticoids	0	4	18	36
%	**0**	**100**	**86**	**84**

FIGURE 4. GCs protect against disease progression and death. Data were analyzed by binomial logistic regression, and the results were reported as OR and 95% CI with the independent variables GC, AA, ACh, 5-HETE, and 11-HETE; the model was adjusted by comorbidity, sex, BMI, and age for groups of patients in different stages of disease. (**A**) Binomial logistic regression analyses considering severity as a dependent variable, with the logistic regression model significant ($p < 0.001$; McFadden $R^2 = 0.73$; Nagelkerke $R^2 = 0.85$; accuracy = 0.93; specificity = 0.93; sensitivity = 0.93; area under the curve = 0.97) in patients with COVID-19 (moderate, $n = 15$; severe, $n = 27$; critical, $n = 22$). (**B**) Binomial logistic regression analyses considering death as a dependent variable, with the logistic regression model significant ($p < 0.001$; McFadden $R^2 = 0.73$; Nagelkerke $R^2 = 0.85$; accuracy = 0.93; specificity = 0.88; sensitivity = 0.97; area under the curve = 0.97) in patients with COVID-19 ($n = 15$ moderate; $n = 27$ severe; $n = 22$ critical). (**C**) GCs prevented death of patients in the severe stage of the disease ($n = 36$ asymptomatic; $n = 50$ moderate; $n = 54$ severe; $n = 55$ critical). (**D**) Plasma ACh levels in patients with severe and critical COVID-19 treated with GCs ($n = 15$ GC discharged; $n = 22$ GC death). Statistics in C were calculated by ANOVA and Mann-Whitney posttest; statistics in D were calculated by Student *t* test; significance was indicated when $p < 0.05$. The bars represent the median ± 95% CI, and the dots represent the data dispersion.

degradation of FAs, sphingolipids, steroid hormones, and vitamin D_3. Linoleic acid, one of the main precursors of AA synthesis in mammals (45), is the best example of FAs whose levels were increased according to COVID-19 severity. The role of AA in COVID-19 is still controversial and poorly understood. Some authors have reported that AA is beneficial to the host because this eicosanoid can induce disturbances in the virus membrane, reducing virus viability and cellular infection (46). Other authors have reported a clear association between low serum levels of AA and enhanced systemic inflammation in deceased patients with COVID-19, suggesting that dysregulated FA/LM levels are related to disease progression (47). Another interesting fact is that sphingolipid-rich microdomains in the epithelial cell membrane regulate the plasma membrane fluidity and facilitate virus fusion and its genome released into the host cell (44). The role of vitamin D_3 in COVID-19 has been widely discussed. Some studies have proposed that vitamin D supplementation is beneficial for patients with COVID-19 because of its anti-inflammatory and antiviral properties (48, 49). However, the vitamin D metabolites $25(OH)D_3$ and 24,25-dihydroxyvitamin D_3 are associated with increased *ALOX5* mRNA expression and 5-lipoxygenase activity (50). The 5-lipoxygenase is an enzyme that can be expressed by activated neutrophils and participates in the synthesis of proinflammatory AA metabolites, such as LTB_4 and 5-HETE, whose levels are heightened in patients with critical COVID-19 (51–53), as described here. Interestingly, we demonstrated that $25(OH)D_3$, $24,25(OH)_2D_3$, and 23S,25,26-trihydroxyvitamin D_3 levels were higher in TAs from severe/critical patients than in critical control participants, reinforcing the concept that vitamin D could be associated with detrimental effects on COVID-19.

We also demonstrated a wide range of LM alteration in TAs of patients with critical COVID-19. More precisely, we detected elevated production of 6-*trans*-LTB_4, PGE_2, TXB_2, and 12-oxo-ETE. Similarly, these metabolites are found in high concentrations in sputum from patients with chronic obstructive pulmonary disease–associated eosinophilic airway inflammation (54). During SARS-CoV-2 infection, cell death generates cell debris and causes a stress response in the endoplasmic reticulum that enhances COX activation (55), but it reduces the activity of 15-hydroxy-PG-dehydrogenase-(NAD^+), an enzyme that degrades PGE_2, with a consequent increase in PGE_2 level (8). PGE_2 acts as a functional amplifier of IL-6 (56) and IL-1β release (10, 57) and may contribute to persistent and exacerbated lung and heart inflammation in patients with COVID-19. However, IL-1β upregulates COX-2 expression and PGE_2 release, indicating that these mediators participate in an inflammation amplification cycle (10, 57, 58). We did not detect differences between TA levels of IL-1β from patients with critical COVID-19 compared with critical control participants. However, we detected a slight increase in plasma levels of IL-1β in patients with COVID-19. Thus, we cannot rule out the participation of IL-1β in the regulation of COX-2 activation in patients with severe COVID-19. Increased IL-1β and PGE_2 promote pulmonary edema, airway obstruction, cell recruitment, and reduced proliferation of human pre-B cells (57, 59–61).

Thrombotic complications and neutrophil extracellular traps are associated with COVID-19 severity (62, 63). In this sense, patients with severe COVID-19 have increased levels of TXB_2, a marker of platelet activation, in plasma and airways (64–66). In addition to platelet hyperreactivity, the enhanced platelet–neutrophil and platelet–monocyte interactions may contribute to poor outcomes in COVID-19 (65, 66). Here, we found increased neutrophil counts in TAs of patients with critical COVID-19 and increased levels of TXB_2. In addition, another upregulated LM in TAs of patients with critical COVID-19 is 6-*trans*-LTB_4, a nonenzymatic degradation product of LTA_4 (67). 6-*Trans*-LTB_4 is detected in high

concentrations in blood from deceased patients with COVID-19 (47). In addition, 6-*trans*-LTB_4 activates neutrophils, increases the expression of ICAM-1 on the cell surface, and promotes their adherence and interaction with endothelial cells, which in turn favors leukocyte infiltration (68). Our results demonstrated that SARS-CoV-2 infection promoted an FA/LM storm linked to the worst COVID-19 outcome. We identified an FA/LM profile associated with disease severity and characterized by a low diversity of mediators with significantly increased concentrations in plasma (AA, 5-HETE, and 11-HETE) and TA samples (AA, 12-oxo-ETE, 5-HETE, 6-*trans*-LTB_4, PGE_2, TXB_2, and 11-HETE). Curiously, Zaid et al. (51) detected significantly high levels of some eicosanoids (12-HHTrE, LTB_4, TXB_2, and PGE_2) in TA from patients with severe COVID-19. Other studies have described FA/LM signatures associated with severe COVID-19 that are composed of a high diversity of molecular species in serum (52) and TA samples (12). The above-mentioned reports indicate a robust correlation between dysregulation of the FA/LM lipidome and COVID-19 severity; however, the differences among these studies may be associated with the use of distinct study designs or experimental approaches, such as type and volume of biological samples, limitations of sensitivity in the detection, and sample processing and extraction procedures. Of note, the inaccessibility of TA samples from healthy subjects restricted our investigation to hospitalized patients with critical COVID-19 and intubated subjects who presented health issues except for COVID-19 (critical control subjects). This limitation may be associated with some data variation in these studies and the low species diversity in the FA/LM signature detected in the biological samples from our patients. The present study reported that SARS-CoV-2 infection induced ACh release at pulmonary and systemic levels and that this effect was more pronounced in the infection site, where the ACh concentration was ~16-fold higher. ACh is produced primarily by the nervous system (16), but lung epithelial cells and leukocytes also release this molecule (17, 69). Neutrophils are important sources of ACh, whose release can be stimulated by LMs such as 11-HETE (70). The 11-HETE is elevated in both the blood and TAs of patients with critical COVID-19. ACh induces mucus secretion, bronchoconstriction, inflammation, lung remodeling (21), cardiac dysfunction (10), and the release of IL-8 (22). An interesting fact is that low ACh concentration was detected in the TA from critical control patients, as opposed to the high concentration detected in patients with critical COVID-19. In critical control participants, this event may be associated with low levels of PGE_2 because this lipid is a strong inducer of ACh (10).

The ACh binding to its receptor triggers the release of AA-derived eicosanoids (71). Indeed, therapies involving nicotinic receptors have been proposed for the treatment of COVID-19 (72) based on the anti-inflammatory effects and the nicotine-mediated desensitization of the ACE2 receptor. Recent studies have reported that nicotine and smoking upregulate ACE2 receptor expression in COVID-19 (73). Therefore, our findings raise concerns for the therapeutic use of nicotinic agonists to treat COVID-19, because patients with severe/critical disease release large amounts of ACh and exhibit increased *CHRM3* gene expression that encodes the cholinergic muscarinic receptor 3. In addition, some authors have proposed the use of AA to treat COVID-19 because of its antiviral and anti-inflammatory effects (46). However, our findings indicate that such a strategy may be inadequate once AA metabolites could favor hyperinflammation and lethality in patients with COVID-19.

A variety of protocols have been proposed as complementary treatments due to the heterogeneous clinical manifestation of COVID-19. In this sense, the effectiveness of GC administration has been reported in hospitalized patients with acute respiratory distress syndrome caused by COVID-19 and patients who receive respiratory support (74). GCs prevent inflammation induced by alveolar damage caused by cytokine and chemokine storms; however, GCs may delay virus elimination and alter lymphocyte proliferation (75) The classically described mechanism of GC action is the inhibition of phospholipase A_2 and COX-2, two enzymes involved in AA metabolism (76). Dexamethasone inhibits PGE_2 synthesis and thus limits ACh release and avoids cardiac dysfunction (10). The reduction of proinflammatory LMs may then explain the clinical benefits of GCs for patients with COVID-19. The GC treatment of patients with severe and critical COVID-19 reduced ACh levels in plasma and TA.

Interestingly, Spearman's correlations detected that the blood levels of AA, 5-HETE, and 11-HETE, as well as ACh, in patients with COVID-19 correlated positively with disease severity, and plasma levels of 5-HETE and ACh correlated positively with days of hospitalization. In TAs, ACh and PGE_2 levels correlated positively and moderately. Circulating neutrophil count levels correlated positively with COVID-19 severity, and neutrophilia is an indicator of severe respiratory symptoms and unfavorable outcomes in COVID-19 (77). As expected, neutrophils were the main cells whose counts were increased in the blood and TAs of patients with severe and critical COVID-19, and here we demonstrated that this phenomenon in blood is associated with lipid storm. Surprisingly, we did not detect a correlation between blood FA/LM and BMI, but elevated levels of AA, 5-HETE, and 12-HETE positively correlated with BMI in TA samples. Obesity is a well-established risk factor for the development of severe forms of COVID-19 (78), a disorder that may favor the generation of persistent inflammation because of increased eicosanoids (79). Taken together, our data demonstrated a correlation between FA/LM, ACh, and clinical markers of COVID-19 at pulmonary and systemic levels, suggesting that these molecules participate in COVID-19 progression.

The logistic regression analysis indicated that high levels of 11-HETE (severity OR, 4.5; death OR, 2.0) tended to be a risk factor for the development of severe forms of COVID-19 and death even after adjusting the model for sex, BMI, comorbidities, and age. In the literature, male sex has been described to be related to the infection rate, severity, and mortality of COVID-19 (80).

Binomial logistic regression analysis demonstrated that administration of GCs protected patients from developing critical forms of COVID-19 and the outcome of death even after adjusting the model for sex, BMI, comorbidities, and age. However, the protective effects of GCs were more prominent in patients with severe disease. In this regard, ~88% of surviving patients with severe COVID-19 were treated with GCs, and only 67% of patients in the critical group experienced recovery with GC therapy (Fig. 4C). This could be explained by the fact that critical patients are in a serious medical condition that causes nonresponsiveness to GC therapy, an event known as the "point of no return" (10, 57). As described here, the RECOVERY clinical trials have also reported that GC therapy reduces the lethality rates more effectively in patients with severe COVID-19 who receive respiratory support than in patients who receive no respiratory support (74). It should be noted that the lethality rates of GC-treated patients with severe COVID-19 in our cohort were higher than those reported in the RECOVERY trial (74). Similarly, the CoDEX trial has reported that GC therapy is useful even when the baseline lethality rate of the participants is high (81). Several reasons could explain this difference, including the low mean partial pressure of oxygen/fraction of inspired oxygen ratio and the burden of the health care system in a resource-limited country such as Brazil (81). Interestingly, these findings corroborate the analysis of binomial logistic regression data about the protective effect of GCs (Fig. 4), which was associated with a reduction of ACh levels. In contrast, the FA/LM levels did not differ significantly between discharged and deceased patients with severe or critical

disease treated or not with GCs. The ineffective response to GC could be associated with the AA production from GC-insensitive sources (82), linoleic acid (83), or enzymatic hydrolysis of endocannabinoids (84, 85). Future investigations are required to clarify the mechanism of the apparent crosstalk between FA/LM and cholinergic mediators in the severity of COVID-19.

Acknowledgments

The authors acknowledge all participants in this study, as well as their families. We also thank the Innovation and Technology Park (Supera); Caroline Fontanari, M.Sc., for her technical and laboratory support; and all professionals of the intensive care unit team and of the Hospital Santa Casa de Misericórdia de Ribeirão Preto and Hospital São Paulo de Ribeirão Preto. The contributions of the Ribeirão Preto Municipal Health Department and the employees of the Serviço de Análises Clínicas of the Faculdade de Ciências Farmacêuticas de Ribeirão Preto, Universidade de São Paulo, were indispensable. We also acknowledge Professors Victor Hugo Aquino Quintana, Ph.D., Márcia Regina von Zeska Kress, Ph.D., and Marcia Eliana da Silva Ferreira, Ph.D., for sharing the BSL2 laboratory. The Visual Abstract was created with BioRender.com (agreement no. KZ23Q982UD).

ImmunoCOVID Brazilian Research Consortium

Ingryd Carmona-Garcia,[1,2] Cristiane M. Milanezi, B.Sc.,[3] Lilian C. Rodrigues, Ph.D.,[1] Cassia F. S. L. Dias, B.Sc.,[1,4] Ana C. Xavier,[5] Giovanna S. Porcel,[5] Isabelle C. Guarneri,[5] Kamila Zaparoli,[6] Caroline T. Garbato,[6] Jamille G. M. Argolo, M.Sc.,[6] Ângelo A. F. Júnior, M.Sc.,[6] Rafael C. da Silva, B.Sc.,[7] Dayane P. da Silva, B.Sc.,[7] Debora C. Nepomuceno, B.Sc.N.,[7] and Rita C. C. Barbieri, B.Sc.N.[8]

[1]Departamento de Análises Clínicas, Toxicológicas e Bromatológicas. Faculdade de Ciências Farmacêuticas de Ribeirão Preto, Universidade de São Paulo, Ribeirão Preto, São Paulo, Brazil; [2]Departamento de Química, Faculdade de Filosofia, Ciências e Letras de Ribeirão Preto, Universidade de São Paulo, Ribeirão Preto, São Paulo, Brazil; [3]Departamento de Bioquímica e Imunologia. Faculdade de Medicina de Ribeirão Preto, Universidade de São Paulo, São Paulo, Brazil; [4]Programa de Pós-Graduação em Biociências e Biotecnologia Aplicadas à Farmácia, Faculdade de Ciências Farmacêuticas de Ribeirão Preto, Universidade de São Paulo, Ribeirão Preto, São Paulo, Brazil; [5]Departamento de Enfermagem Materno-Infantil e Saúde Pública, Escola de Enfermagem de Ribeirão Preto, Universidade de São Paulo, Ribeirão Preto, São Paulo, Brazil; [6]Departamento de Enfermagem Geral e Especializada, Escola de Enfermagem de Ribeirão Preto, Universidade de São Paulo, Ribeirão Preto, São Paulo, Brazil; [7]Hospital Santa Casa de Misericórdia de Ribeirão Preto, Ribeirão Preto, São Paulo, Brazil; [8]Hospital São Paulo, Ribeirão Preto, São Paulo, Brazil

Disclosures

The authors have no financial conflicts of interest.

References

1. Huang, C., Y. Wang, X. Li, L. Ren, J. Zhao, Y. Hu, L. Zhang, G. Fan, J. Xu, X. Gu, et al. 2020. Clinical features of patients infected with 2019 novel coronavirus in Wuhan, China. *Lancet* 395: 497–506.
2. Hu, B., S. Huang, and L. Yin. 2021. The cytokine storm and COVID-19. *J. Med. Virol.* 93: 250–256.
3. Nienhold, R., Y. Ciani, V. H. Koelzer, A. Tzankov, J. D. Haslbauer, T. Menter, N. Schwab, M. Henkel, A. Frank, V. Zsikla, et al. 2020. Two distinct immunopathological profiles in autopsy lungs of COVID-19. *Nat. Commun.* 11: 5086.
4. Desai, N., A. Neyaz, A. Szabolcs, A. R. Shih, J. H. Chen, V. Thapar, L. T. Nieman, A. Solovyov, A. Mehta, D. J. Lieb, et al. 2020. Temporal and spatial heterogeneity of host response to SARS-CoV-2 pulmonary infection. *Nat. Commun.* 11: 6319.
5. Grant, R. A., L. Morales-Nebreda, N. S. Markov, S. Swaminathan, M. Querrey, E. R. Guzman, D. A. Abbott, H. K. Donnelly, A. Donayre, I. A. Goldberg, et al; NU SCRIPT Study Investigators. 2021. Circuits between infected macrophages and T cells in SARS-CoV-2 pneumonia. *Nature* 590: 635–641.
6. Damiani, S., M. Fiorentino, A. De Palma, M. P. Foschini, T. Lazzarotto, L. Gabrielli, P. L. Viale, L. Attard, M. Riefolo, and A. D'Errico. 2021. Pathological post-mortem findings in lungs infected with SARS-CoV-2. *J. Pathol.* 253: 31–40.
7. Sanak, M. 2016. Eicosanoid mediators in the airway inflammation of asthmatic patients: what is new? *Allergy Asthma Immunol. Res.* 8: 481–490.
8. Dennis, E. A., and P. C. Norris. 2015. Eicosanoid storm in infection and inflammation. [Published erratum appears in 2015 Nat. Rev. Immunol. 15: 724.] *Nat. Rev. Immunol.* 15: 511–523.
9. Esser-von Bieren, J. 2017. Immune-regulation and -functions of eicosanoid lipid mediators. *Biol. Chem.* 398: 1177–1191.
10. Reis, M. B., F. L. Rodrigues, N. Lautherbach, A. Kanashiro, C. A. Sorgi, A. F. G. Meirelles, C. A. A. Silva, K. F. Zoccal, C. O. S. Souza, S. G. Ramos, et al. 2020. Interleukin-1 receptor-induced PGE_2 production controls acetylcholine-mediated cardiac dysfunction and mortality during scorpion envenomation. *Nat. Commun.* 11: 5433.
11. Kolmert, J., C. Gómez, D. Balgoma, M. Sjödin, J. Bood, J. R. Konradsen, M. Ericsson, J. O. Thörngren, A. James, M. Mikus, et al; U-BIOPRED Study Group, on behalf of the U-BIOPRED Study Group. 2021. Urinary leukotriene E_4 and prostaglandin D_2 metabolites increase in adult and childhood severe asthma characterized by type 2 inflammation. A clinical observational study. *Am. J. Respir. Crit. Care Med.* 203: 37–53.
12. Archambault, A. S., Y. Zaid, V. Rakotoarivelo, C. Turcotte, É. Doré, I. Dubuc, C. Martin, O. Flamand, Y. Amar, A. Cheikh, et al. 2021. High levels of eicosanoids and docosanoids in the lungs of intubated COVID-19 patients. *FASEB J.* 35: e21666.
13. Aradhyula, V., E. Waigi, N. R. Bearss, J. M. Edwards, B. Joe, C. G. McCarthy, L. B. Koch, and C. F. Wenceslau. 2021. Intrinsic exercise capacity induces divergent vascular plasticity via arachidonic acid-mediated inflammatory pathways in female rats. *Vascul. Pharmacol.* 140: 106862.
14. Angelini, P. 2019. An unusual case of takotsubo cardiomyopathy in pheochromocytoma. *Tex. Heart Inst. J.* 46: 128–129.
15. Minhas, A. S., P. Scheel, B. Garibaldi, G. Liu, M. Horton, M. Jennings, S. R. Jones, E. D. Michos, and A. G. Hays. 2020. Takotsubo syndrome in the setting of COVID-19. *JACC. Case Rep.* 2: 1321–1325.
16. McGovern, A. E., and S. B. Mazzone. 2014. Neural regulation of inflammation in the airways and lungs. *Auton. Neurosci.* 182: 95–101.
17. Wessler, I., and C. J. Kirkpatrick. 2020. Cholinergic signaling controls immune functions and promotes homeostasis. *Int. Immunopharmacol.* 83: 106345.
18. Proskocil, B. J., H. S. Sekhon, Y. Jia, V. Savchenko, R. D. Blakely, J. Lindstrom, and E. R. Spindel. 2004. Acetylcholine is an autocrine or paracrine hormone synthesized and secreted by airway bronchial epithelial cells. *Endocrinology* 145: 2498–2506.
19. Chang, E. H., S. S. Chavan, and V. A. Pavlov. 2019. Cholinergic control of inflammation, metabolic dysfunction, and cognitive impairment in obesity-associated disorders: mechanisms and novel therapeutic opportunities. *Front. Neurosci.* 13: 263.
20. Roy, A., S. Guatimosim, V. F. Prado, R. Gros, and M. A. M. Prado. 2015. Cholinergic activity as a new target in diseases of the heart. *Mol. Med.* 20: 527–537.
21. Kistemaker, L. E. M., and R. Gosens. 2015. Acetylcholine beyond bronchoconstriction: roles in inflammation and remodeling. *Trends Pharmacol. Sci.* 36: 164–171.
22. Profita, M., A. Bonanno, L. Siena, M. Ferraro, A. M. Montalbano, F. Pompeo, L. Riccobono, M. P. Pieper, and M. Gjomarkaj. 2008. Acetylcholine mediates the release of IL-8 in human bronchial epithelial cells by a NFκB/ERK-dependent mechanism. *Eur. J. Pharmacol.* 582: 145–153.
23. Shields, M. D., and J. Riedler. 2000. Bronchoalveolar lavage and tracheal aspirate for assessing airway inflammation in children. *Am. J. Respir. Crit. Care Med.* 162(Suppl 1):S15–S17.
24. Sorgi, C. A., A. P. F. Peti, T. Petta, A. F. G. Meirelles, C. Fontanari, L. A. B. Moraes, and L. H. Faccioli. 2018. Comprehensive high-resolution multiple-reaction monitoring mass spectrometry for targeted eicosanoid assays. *Sci. Data* 5: 180167.
25. Pereira, P. A. T., C. S. Bitencourt, M. B. Reis, F. G. Frantz, C. A. Sorgi, C. O. S. Souza, C. L. Silva, L. G. Gardinassi, and L. H. Faccioli. 2020. Immunomodulatory activity of hyaluronidase is associated with metabolic adaptations during acute inflammation. *Inflamm. Res.* 69: 105–113.
26. Santos-Lobato, B. L., L. G. Gardinassi, M. Bortolanza, A. P. F. Peti, Â. V. Pimentel, L. H. Faccioli, E. A. Del-Bel, and V. Tumas. 2022. Metabolic profile in plasma and CSF of levodopa-induced dyskinesia in Parkinson's disease: focus on neuroinflammation. *Mol. Neurobiol.* 59: 1140–1150.
27. Chambers, M. C., B. Maclean, R. Burke, D. Amodei, D. L. Ruderman, S. Neumann, L. Gatto, B. Fischer, B. Pratt, J. Egertson, et al. 2012. A cross-platform toolkit for mass spectrometry and proteomics. *Nat. Biotechnol.* 30: 918–920.
28. Yu, T., Y. Park, J. M. Johnson, and D. P. Jones. 2009. apLCMS—adaptive processing of high-resolution LC/MS data. *Bioinformatics* 25: 1930–1936.
29. Li, S., Y. Park, S. Duraisingham, F. H. Strobel, N. Khan, Q. A. Soltow, D. P. Jones, and B. Pulendran. 2013. Predicting network activity from high throughput metabolomics. *PLOS Comput. Biol.* 9: e1003123.
30. Overmyer, K. A., E. Shishkova, I. J. Miller, J. Balnis, M. N. Bernstein, T. M. Peters-Clarke, J. G. Meyer, Q. Quan, L. K. Muehlbauer, E. A. Trujillo, et al. 2021. Large-scale multi-omic analysis of COVID-19 severity. *Cell Syst.* 12: 23–40.e7.
31. Batabyal, R., N. Freishtat, E. Hill, M. Rehman, R. Freishtat, and I. Koutroulis. 2021. Metabolic dysfunction and immunometabolism in COVID-19 pathophysiology and therapeutics. *Int. J. Obes.* 45: 1163–1169.
32. Wong, S. L., F. P. Leung, C. W. Lau, C. L. Au, L. M. Yung, X. Yao, Z. Y. Chen, P. M. Vanhoutte, M. Gollasch, and Y. Huang. 2009. Cyclooxygenase-2-derived prostaglandin $F_{2\alpha}$ mediates endothelium-dependent contractions in the aortae of hamsters with increased impact during aging. *Circ. Res.* 104: 228–235.
33. Edwards, J. M., C. G. McCarthy, and C. F. Wenceslau. 2020. The obligatory role of the acetylcholine-induced endothelium-dependent contraction in hypertension: can arachidonic acid resolve this inflammation? *Curr. Pharm. Des.* 26: 3723–3732.
34. Jenkins, B., E. de Schryver, P. P. Van Veldhoven, and A. Koulman. 2017. Peroxisomal 2-hydroxyacyl-CoA lyase is involved in endogenous biosynthesis of heptadecanoic acid. *Molecules* 22: 1718.
35. Thomas, T., D. Stefanoni, J. A. Reisz, T. Nemkov, L. Bertolone, R. O. Francis, K. E. Hudson, J. C. Zimring, K. C. Hansen, E. A. Hod, et al. 2020. COVID-19

infection alters kynurenine and fatty acid metabolism, correlating with IL-6 levels and renal status. *JCI Insight* 5: e140327.
36. Heffernan, K. S., S. M. Ranadive, and S. Y. Jae. 2020. Exercise as medicine for COVID-19: on PPAR with emerging pharmacotherapy. *Med. Hypotheses* 143: 110197.
37. Venn-Watson, S., R. Lumpkin, and E. A. Dennis. 2020. Efficacy of dietary odd-chain saturated fatty acid pentadecanoic acid parallels broad associated health benefits in humans: could it be essential? *Sci. Rep.* 10: 8161.
38. Yao, J., J. Yan, J. Wu, J. Yu, B. He, X. Chen, and Z. Chen. 2021. Predicting target genes of San-Huang-Chai-Zhu formula in treating ANIT-induced acute intrahepatic cholestasis rat model via bioinformatics analysis combined with experimental validation. *Evid. Based Complement. Alternat. Med.* 2021: 5320445.
39. Wang, Q., Y. He, Y. Shen, Q. Zhang, D. Chen, C. Zuo, J. Qin, H. Wang, J. Wang, and Y. Yu. 2014. Vitamin D inhibits COX-2 expression and inflammatory response by targeting thioesterase superfamily member 4. *J. Biol. Chem.* 289: 11681–11694.
40. Maeda, S., Q. Qu, M. J. Robertson, G. Skiniotis, and B. K. Kobilka. 2019. Structures of the M1 and M2 muscarinic acetylcholine receptor/G-protein complexes. *Science* 364: 552–557.
41. Waldo, G. L., T. K. Ricks, S. N. Hicks, M. L. Cheever, T. Kawano, K. Tsuboi, X. Wang, C. Montell, T. Kozasa, J. Sondek, and T. K. Harden. 2010. Kinetic scaffolding mediated by a phospholipase C-β and Gq signaling complex. *Science* 330: 974–980.
42. Balsinde, J., E. Diez, and F. Mollinedo. 1991. Arachidonic acid release from diacylglycerol in human neutrophils. Translocation of diacylglycerol-deacylating enzyme activities from an intracellular pool to plasma membrane upon cell activation. *J. Biol. Chem.* 266: 15638–15643.
43. Li, Y., Y. Zhang, R. Lu, M. Dai, M. Shen, J. Zhang, Y. Cui, B. Liu, F. Lin, L. Chen, et al. 2021. Lipid metabolism changes in patients with severe COVID-19. *Clin. Chim. Acta* 517: 66–73.
44. Abu-Farha, M., T. A. Thanaraj, M. G. Qaddoumi, A. Hashem, J. Abubaker, and F. Al-Mulla. 2020. The role of lipid metabolism in COVID-19 virus infection and as a drug target. *Int. J. Mol. Sci.* 21: 3544.
45. Le, H. D., J. A. Meisel, V. E. de Meijer, K. M. Gura, and M. Puder. 2009. The essentiality of arachidonic acid and docosahexaenoic acid. *Prostaglandins Leukot. Essent. Fatty Acids* 81: 165–170.
46. Das, U. N. 2020. Can bioactive lipids inactivate coronavirus (COVID-19)? *Arch. Med. Res.* 51: 282–286.
47. Palmas, F., J. Clarke, R. A. Colas, E. A. Gomez, A. Keogh, M. Boylan, N. McEvoy, O. J. McElvaney, O. McElvaney, R. Alalqam, et al. 2021. Dysregulated plasma lipid mediator profiles in critically ill COVID-19 patients. *PLoS One* 16: e0256226.
48. Martineau, A. R., and N. G. Forouhi. 2020. Vitamin D for COVID-19: a case to answer? *Lancet Diabetes Endocrinol.* 8: 735–736.
49. Murdaca, G., G. Pioggia, and S. Negrini. 2020. Vitamin D and Covid-19: an update on evidence and potential therapeutic implications. *Clin. Mol. Allergy* 18: 23.
50. Somjen, D., S. Katzburg, M. Grafi-Cohen, E. Knoll, O. Sharon, and G. H. Posner. 2011. Vitamin D metabolites and analogs induce lipoxygenase mRNA expression and activity as well as reactive oxygen species (ROS) production in human bone cell line. *J. Steroid Biochem. Mol. Biol.* 123: 85–89.
51. Zaid, Y., É. Doré, I. Dubuc, A. S. Archambault, O. Flamand, M. Laviolette, N. Flamand, É. Boilard, and L. Flamand. 2021. Chemokines and eicosanoids fuel the hyperinflammation within the lungs of patients with severe COVID-19. *J. Allergy Clin. Immunol.* 148: 368–380.e3.
52. Schwarz, B., L. Sharma, L. Roberts, X. Peng, S. Bermejo, I. Leighton, A. Casanovas-Massana, M. Minasyan, S. Farhadian, A. I. Ko, et al; Yale IMPACT Team. 2021. Cutting edge: severe SARS-CoV-2 infection in humans is defined by a shift in the serum lipidome, resulting in dysregulation of eicosanoid immune mediators. *J. Immunol.* 206: 329–334.
53. Zschaler, J., and J. Arnhold. 2016. Impact of simultaneous stimulation of 5-lipoxygenase and myeloperoxidase in human neutrophils. *Prostaglandins Leukot. Essent. Fatty Acids* 107: 12–21.
54. Celejewska-Wójcik, N., A. Kania, K. Górka, P. Nastałek, K. Wójcik, A. Gielicz, L. Mastalerz, M. Sanak, and K. Sładek. 2021. Eicosanoids and eosinophilic inflammation of airways in stable COPD. *Int. J. Chron. Obstruct. Pulmon. Dis.* 16: 1415–1424.
55. Hammock, B. D., W. Wang, M. M. Gilligan, and D. Panigrahy. 2020. Eicosanoids: the overlooked storm in coronavirus disease 2019 (COVID-19)? *Am. J. Pathol.* 190: 1782–1788.
56. Caselli, G., A. Bonazzi, M. Lanza, F. Ferrari, D. Maggioni, C. Ferioli, R. Giambelli, E. Comi, S. Zerbi, M. Perrella, et al. 2018. Pharmacological characterisation of CR6086, a potent prostaglandin E_2 receptor 4 antagonist, as a new potential disease-modifying anti-rheumatic drug. *Arthritis Res. Ther.* 20: 39.
57. Zoccal, K. F., C. A. Sorgi, J. I. Hori, F. W. G. Paula-Silva, E. C. Arantes, C. H. Serezani, D. S. Zamboni, and L. H. Faccioli. 2016. Opposing roles of LTB4 and PGE2 in regulating the inflammasome-dependent scorpion venom-induced mortality. *Nat. Commun.* 7: 10760.
58. Mitchell, J. A., M. G. Belvisi, P. Akarasereenont, R. A. Robbins, O. J. Kwon, J. Croxtall, P. J. Barnes, and J. R. Vane. 1994. Induction of cyclo-oxygenase-2 by cytokines in human pulmonary epithelial cells: regulation by dexamethasone. *Br. J. Pharmacol.* 113: 1008–1014.
59. Gross, S., P. Tilly, D. Hentsch, J. L. Vonesch, and J. E. Fabre. 2007. Vascular wall-produced prostaglandin E2 exacerbates arterial thrombosis and atherothrombosis through platelet EP3 receptors. *J. Exp. Med.* 204: 311–320.
60. Ripon, M. A. R., D. R. Bhowmik, M. T. Amin, and M. S. Hossain. 2021. Role of arachidonic cascade in COVID-19 infection: a review. *Prostaglandins Other Lipid Mediat.* 154: 106539.
61. Rider, P., Y. Carmi, O. Guttman, A. Braiman, I. Cohen, E. Voronov, M. R. White, C. A. Dinarello, and R. N. Apte. 2011. IL-1α and IL-1β recruit different myeloid cells and promote different stages of sterile inflammation. *J. Immunol.* 187: 4835–4843.
62. Connors, J. M., and J. H. Levy. 2020. COVID-19 and its implications for thrombosis and anticoagulation. *Blood* 135: 2033–2040.
63. Middleton, E. A., X. Y. He, F. Denorme, R. A. Campbell, D. Ng, S. P. Salvatore, M. Mostyka, A. Baxter-Stoltzfus, A. C. Borczuk, M. Loda, et al. 2020. Neutrophil extracellular traps contribute to immunothrombosis in COVID-19 acute respiratory distress syndrome. *Blood* 136: 1169–1179.
64. Zaid, Y., F. Guessous, F. Puhm, W. Elhamdani, L. Chentoufi, A. C. Morris, A. Cheikh, F. Jalali, E. Boilard, and L. Flamand. 2021. Platelet reactivity to thrombin differs between patients with COVID-19 and those with ARDS unrelated to COVID-19. *Blood Adv.* 5: 635–639.
65. Manne, B. K., F. Denorme, E. A. Middleton, I. Portier, J. W. Rowley, C. Stubben, A. C. Petrey, N. D. Tolley, L. Guo, M. Cody, et al. 2020. Platelet gene expression and function in patients with COVID-19. *Blood* 136: 1317–1329.
66. Hottz, E. D., I. G. Azevedo-Quintanilha, L. Palhinha, L. Teixeira, E. A. Barreto, C. R. R. Pão, C. Righy, S. Franco, T. M. L. Souza, P. Kurtz, et al. 2020. Platelet activation and platelet-monocyte aggregate formation trigger tissue factor expression in patients with severe COVID-19. *Blood* 136: 1330–1341.
67. Borgeat, P., and B. Samuelsson. 1979. Metabolism of arachidonic acid in polymorphonuclear leukocytes. Structural analysis of novel hydroxylated compounds. *J. Biol. Chem.* 254: 7865–7869.
68. Eun, J. C., E. E. Moore, A. Banerjee, M. R. Kelher, S. Y. Khan, D. J. Elzi, N. J. D. McLaughlin, and C. C. Silliman. 2011. Leukotriene B_4 and its metabolites prime the neutrophil oxidase and induce proinflammatory activation of human pulmonary microvascular endothelial cells. *Shock* 35: 240–244.
69. Neumann, S., M. Razen, P. Habermehl, C. U. Meyer, F. Zepp, C. J. Kirkpatrick, and I. Wessler. 2007. The non-neuronal cholinergic system in peripheral blood cells: effects of nicotinic and muscarinic receptor antagonists on phagocytosis, respiratory burst and migration. *Life Sci.* 80: 2361–2364.
70. Gauthier, K. M., D. H. Goldman, N. T. Aggarwal, Y. Chawengsub, J. R. Falck, and W. B. Campbell. 2011. Role of arachidonic acid lipoxygenase metabolites in acetylcholine-induced relaxations of mouse arteries. *Am. J. Physiol. Heart Circ. Physiol.* 300: H725–H735.
71. Vijayaraghavan, S., B. Huang, E. M. Blumenthal, and D. K. Berg. 1995. Arachidonic acid as a possible negative feedback inhibitor of nicotinic acetylcholine receptors on neurons. *J. Neurosci.* 15: 3679–3687.
72. Changeux, J. P., Z. Amoura, F. A. Rey, and M. Miyara. 2020. A nicotinic hypothesis for Covid-19 with preventive and therapeutic implications. *C. R. Biol.* 343: 33–39.
73. Leung, J. M., C. X. Yang, D. D. Sin. 2020. COVID-19 and nicotine as a mediator of ACE-2. *Eur. Respir. J.* 55: 2001261.
74. RECOVERY Collaborative Group. 2021. Dexamethasone in hospitalized patients with Covid-19. *N. Engl. J. Med.* 384: 693–704.
75. Russell, C. D., J. E. Millar, and J. K. Baillie. 2020. Clinical evidence does not support corticosteroid treatment for 2019-nCoV lung injury. *Lancet* 395: 473–475.
76. Rhen, T., and J. A. Cidlowski. 2005. Antiinflammatory action of glucocorticoids—new mechanisms for old drugs. *N. Engl. J. Med.* 353: 1711–1723.
77. Singh, K., S. Mittal, S. Gollapudi, A. Butzmann, J. Kumar, and R. S. Ohgami. 2021. A meta-analysis of SARS-CoV-2 patients identifies the combinatorial significance of D-dimer, C-reactive protein, lymphocyte, and neutrophil values as a predictor of disease severity. *Int. J. Lab. Hematol.* 43: 324–328.
78. Popkin, B. M., S. Du, W. D. Green, M. A. Beck, T. Algaith, C. H. Herbst, R. F. Alsukait, M. Alluhidan, N. Alazemi, and M. Shekar. 2020. Individuals with obesity and COVID-19: a global perspective on the epidemiology and biological relationships. *Obes. Rev.* 21: e13128.
79. Hardwick, J. P., K. Eckman, Y. K. Lee, M. A. Abdelmegeed, A. Esterle, W. M. Chilian, J. Y. Chiang, and B. J. Song. 2013. Eicosanoids in metabolic syndrome. *Adv. Pharmacol.* 66: 157–266.
80. Jun, T., S. Nirenberg, T. Weinberger, N. Sharma, E. Pujadas, C. Cordon-Cardo, P. Kovatch, and K. Huang. 2021. Analysis of sex-specific risk factors and clinical outcomes in COVID-19. *Commun. Med. (Lond.)* 1: 3.
81. Tomazini, B. M., I. S. Maia, A. B. Cavalcanti, O. Berwanger, R. G. Rosa, V. C. Veiga, A. Avezum, R. D. Lopes, F. R. Bueno, M. V. A. O. Silva, et al; COALITION COVID-19 Brazil III Investigators. 2020. Effect of dexamethasone on days alive and ventilator-free in patients with moderate or severe acute respiratory distress syndrome and COVID-19: the CoDEX randomized clinical trial. *JAMA* 324: 1307–1316.
82. Kobza Black, A., M. W. Greaves, and C. N. Hensby. 1982. The effect of systemic prednisolone on arachidonic acid, and prostaglandin E2 and F2 alpha levels in human cutaneous inflammation. *Br. J. Clin. Pharmacol.* 14: 391–394.
83. Alzoghaibi, M. A., S. W. Walsh, A. Willey, D. R. Yager, A. A. Fowler III, and M. F. Graham. 2004. Linoleic acid induces interleukin-8 production by Crohn's human intestinal smooth muscle cells via arachidonic acid metabolites. *Am. J. Physiol. Gastrointest. Liver Physiol.* 286: G528–G537.
84. Dinh, T. P., D. Carpenter, F. M. Leslie, T. F. Freund, I. Katona, S. L. Sensi, S. Kathuria, and D. Piomelli. 2002. Brain monoglyceride lipase participating in endocannabinoid inactivation. [Published erratum appears in 2002 *Proc. Natl. Acad. Sci. U. S. A.* 99: 13961.] *Proc. Natl. Acad. Sci. U. S. A.* 99: 10819–10824.
85. Cravatt, B. F., D. K. Giang, S. P. Mayfield, D. L. Boger, R. A. Lerner, and N. B. Gilula. 1996. Molecular characterization of an enzyme that degrades neuromodulatory fatty-acid amides. *Nature* 384: 83–87.